

## RESEARCH ARTICLE SUMMARY

## HUMAN GENETICS

# Heart-brain connections: Phenotypic and genetic insights from magnetic resonance images

Bingxin Zhao, Tengfei Li, Zirui Fan, Yue Yang, Juan Shu, Xiaochen Yang, Xifeng Wang, Tianyou Luo, Jiarui Tang, Di Xiong, Zhenyi Wu, Bingxuan Li, Jie Chen, Yue Shan, Chalmer Tomlinson, Ziliang Zhu, Yun Li, Jason L. Stein, Hongtu Zhu\*

**INTRODUCTION:** There is increasing evidence pointing to a close relationship between heart health and brain health, with cardiovascular diseases potentially leading to brain diseases such as stroke, dementia, and cognitive impairment. Magnetic resonance imaging (MRI) is a valuable tool that can be used to assess both the heart and brain, generating biomarkers and endophenotypes for various clinical outcomes. However, although recent large-scale analyses have been conducted on heart and brain MRI-derived traits separately, few studies have explored the potential for multi-

organ MRI to examine heart-brain connections and identify shared genetic effects. The structural and functional links between the heart and the brain remain unclear.

**RATIONALE:** Using multiorgan MRI and genetic data from >40,000 subjects, we aimed to quantify interorgan connections between the heart and brain and identify the underlying genetic variants. Specifically, we analyzed 82 cardiac and aortic MRI-derived traits across six categories: left and right ventricles, left and right atria, and ascending and descending aortas, as

well as 458 brain MRI traits that measured structure and function.

**RESULTS:** After controlling for various covariates, we found that heart MRI traits were clearly associated with the brain across all imaging modalities studied. We observed multiple patterns of association for brain gray matter morphometry, white matter microstructure, and functional networks. For example, we found that the left ventricle of the heart showed the strongest correlations with microstructure metrics of cerebral white matter tracts, suggesting that adverse heart features were associated with poorer white matter microstructure.

Our genome-wide association analysis of heart MRI traits identified 80 associated genomic loci ( $P < 6.09 \times 10^{-10}$ ). We performed sex-specific analysis and found that the genetic effects on heart structure and function were highly consistent between both sexes. Further, we conducted a systematic search of previously reported genetic results in these genomic loci and found that heart MRI traits had shared genetic influences and colocalized with heart and brain diseases and complex traits.

We identified genetic correlations between heart MRI traits and various brain complex traits and diseases such as stroke, eating disorders, schizophrenia, cognitive function, and mental health traits. For example, adverse myocardial wall thickness condition was positively genetically correlated with stroke. We further used two-sample Mendelian randomization to explore causal genetic links between the heart and brain, and our findings suggest that adverse heart features have genetic causal effects on several brain diseases such as psychiatric disorders and depression.

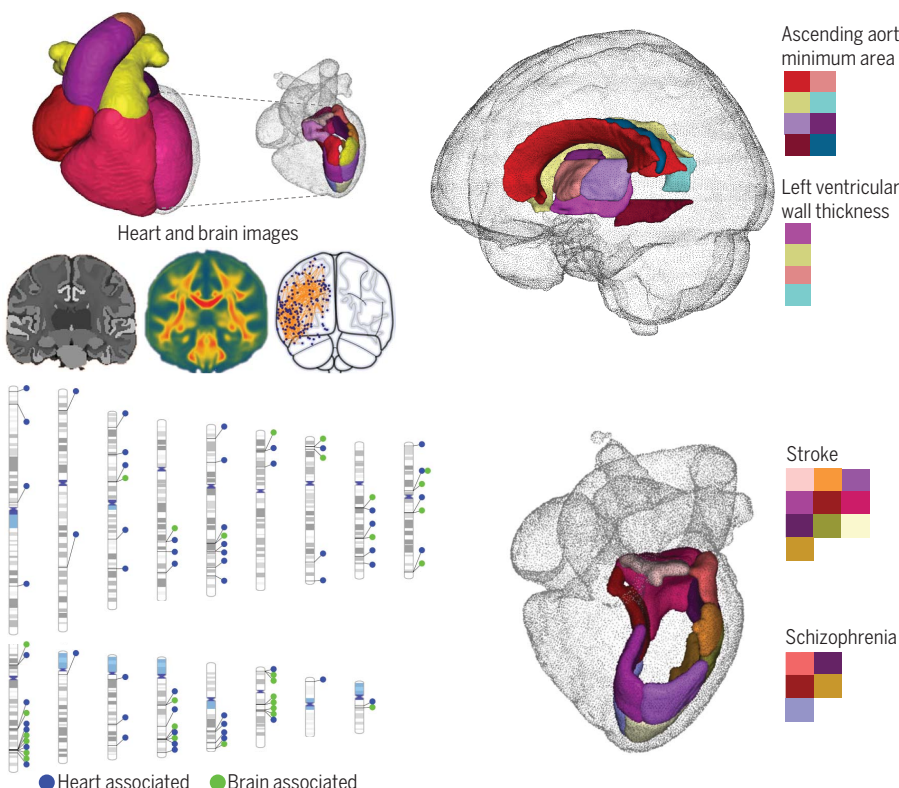
**CONCLUSION:** This study deepened our understanding of heart-brain links and their genetic basis. We observed that MRI measurements of the two organs were associated with each other, and this was independent of a wide variety of body measures, shared risk factors, and imaging confounders. We also uncovered genetic colocalizations and correlations between heart structure and function and brain clinical end points, suggesting that adverse heart metrics may have implications for brain abnormalities and the risk of brain diseases. By understanding human health from a multiorgan perspective, we may be able to improve disease risk prediction and prevention and mitigate the negative effects of one organ disease on other organs that may be at risk. ■

The list of author affiliations is available in the full article online.

\*Corresponding author. Email: htzhu@email.unc.edu

Cite this article as B. Zhao et al., *Science* **380**, eabn6598 (2023). DOI: 10.1126/science.abn6598

**S** READ THE FULL ARTICLE AT  
<https://doi.org/10.1126/science.abn6598>



**Heart-brain connections revealed by multiorgan imaging genetics.** Top left: Quantifying the heart and brain structure and function in MRI. Top right: Examples of associations between heart MRI traits and brain white matter tracts. Bottom left: Genomic loci associated with heart MRI traits that overlapped with traits and disorders of the heart and/or brain. Bottom right: Selected genetic correlations between heart MRI traits and brain disorders.

## RESEARCH ARTICLE

## HUMAN GENETICS

# Heart-brain connections: Phenotypic and genetic insights from magnetic resonance images

Bingxin Zhao<sup>1,2</sup>, Tengfei Li<sup>3,4</sup>, Zirui Fan<sup>1,2</sup>, Yue Yang<sup>5</sup>, Juan Shu<sup>2</sup>, Xiaochen Yang<sup>2</sup>, Xifeng Wang<sup>5</sup>, Tianyou Luo<sup>5</sup>, Jiarui Tang<sup>5</sup>, Di Xiong<sup>5</sup>, Zhenyi Wu<sup>2</sup>, Bingxuan Li<sup>6</sup>, Jie Chen<sup>5</sup>, Yue Shan<sup>5</sup>, Chalmer Tomlinson<sup>5</sup>, Ziliang Zhu<sup>5</sup>, Yun Li<sup>5,7</sup>, Jason L. Stein<sup>7,8</sup>, Hongtu Zhu<sup>4,5,7,9,10\*</sup>

Cardiovascular health interacts with cognitive and mental health in complex ways, yet little is known about the phenotypic and genetic links of heart-brain systems. We quantified heart-brain connections using multiorgan magnetic resonance imaging (MRI) data from more than 40,000 subjects. Heart MRI traits displayed numerous association patterns with brain gray matter morphometry, white matter microstructure, and functional networks. We identified 80 associated genomic loci ( $P < 6.09 \times 10^{-10}$ ) for heart MRI traits, which shared genetic influences with cardiovascular and brain diseases. Genetic correlations were observed between heart MRI traits and brain-related traits and disorders. Mendelian randomization suggests that heart conditions may causally contribute to brain disorders. Our results advance a multiorgan perspective on human health by revealing heart-brain connections and shared genetic influences.

**A** growing amount of evidence suggests close interplays between heart health and brain health (fig. S1). Cardiovascular diseases may provide a pathophysiological background for several brain diseases, including stroke (1), dementia (2), cerebral small vessel disease (3), and cognitive impairment (4, 5). For example, atrial fibrillation has been linked to an increased incidence of dementia (6) and silent cerebral damage (7) even in stroke-free cohorts (8). It has been consistently observed that heart failure is associated with cognitive impairment and eventually dementia (9), likely because of the reduced cerebral perfusion caused by the failing heart (10). Conversely, mental disorders and negative psychological factors may contribute substantially to the initiation and progression of cardiovascular diseases (11–13). Patients with mental illnesses such as schizophrenia, bipolar disorder, epilepsy, or depression show an increased incidence of cardiovascular diseases (14–17). Acute mental stress may cause a higher risk of atheros-

sclerosis because of stress-induced vascular inflammation and leukocyte migration (18). Primarily because of the lack of data, almost all prior studies on heart-brain interactions and associated risk factors (19–25) have focused on one (or a few) specific diseases or used small samples. Therefore, the overall picture of the structural and functional links between the heart and the brain remains unclear.

In heart and brain diseases, magnetic resonance imaging (MRI)-derived traits are well-established endophenotypes. Cardiovascular magnetic resonance imaging (CMR) has been widely used to assess cardiac structure and function, yielding insights into the risk and pathological status of cardiovascular diseases (26–28). Brain MRI modalities provide detailed information about brain structure and function (29). Clinical applications of brain MRI have revealed the associated brain abnormalities that accompany multiple neurological and neuropsychiatric disorders (30–32). Moreover, twin and family studies have shown that CMR and brain MRI traits are moderately to highly heritable (33–35). For example, the left ventricular mass (LVM) has a heritability estimate  $>0.8$  (34). Most brain structural MRI traits are highly heritable (heritability ranges from 0.6 to 0.8) (36), and the heritability of brain functional connectivity is usually between 0.2 and 0.6 (37). A few recent genome-wide association studies (GWAS) have been separately conducted on CMR (38–43) and brain MRI traits (44–51). For example, several large-scale efforts have been made to discover genetic variants associated with brain structures; examples include ENIGMA (31), Neuro-CHARGE (52), and IMAGEN (53). Although MRI has been widely used in clinical research

and genetic mapping, few studies have used multiorgan MRI to examine heart-brain connections and identify the shared genetic signatures of the heart and the brain.

In the present study, we investigated heart-brain connections using multiorgan imaging data obtained from >40,000 subjects in the UK Biobank (UKB) study (54). By using a recently developed heart segmentation and feature extraction pipeline (55–57), we generated 82 CMR traits from the raw short-axis, long-axis, and aortic cine images. These CMR traits included global measures of four cardiac chambers, the left ventricle (LV), right ventricle (RV), left atrium (LA), and right atrium (RA), and two aortic sections, the ascending aorta (AAo) and the descending aorta (DAO), as well as regional (58) phenotypes of the LV myocardial wall thickness and strain [table S1 and supplementary text (59)]. Then, we identified the relationships between the 82 CMR traits and a wide variety of the brain MRI traits discovered from multimodality images (60), including structural MRI (164 traits), diffusion MRI (110 traits), resting functional MRI (resting fMRI) (92 global traits and >60,000 regional traits), and task fMRI (92 global traits and >60,000 regional traits). These brain MRI traits provided fine details of brain structural morphometry (45, 61) (regional brain volumes and cortical thickness traits), brain structural connectivity (47, 62) [diffusion tensor imaging (DTI) invariant measures of white matter tracts], and brain intrinsic and extrinsic functional organizations (49, 63, 64) (functional activity and connectivity at rest and during a task) (table S2). To evaluate the genetic determinants underlying heart-brain connections, we performed GWASs for the 82 CMR traits to uncover the genetic architecture of the heart and aorta. Compared with existing GWASs of CMR traits (38–43), our study used a much broader group of cardiac and aortic traits, allowing us to identify the shared genetic components with a wide variety of brain-related complex traits and disorders. For example, (42) mainly focused on nine measures of the right heart, (38) analyzed six LV traits, and (43) studied three traits of diastolic function. Figure 1 provides an overview of the study design and analyses. The GWAS results of 82 CMR traits can be explored and are freely available through the heart imaging genetics knowledge portal (Heart-KP) at <http://heartkp.org/>.

## Phenotypic heart-brain connections

To verify that the 82 CMR traits are well defined and biologically meaningful, we first examined their reproducibility using the repeat scans obtained from the UKB repeat imaging visit ( $n = 2903$ ; average time between visits, 2 years). For each trait, we calculated the intra-class correlation (ICC) between two observations from all revisited individuals. The average ICC was 0.653 (range = 0.369 to 0.970; table S1).

<sup>1</sup>Department of Statistics and Data Science, University of Pennsylvania, Philadelphia, PA 19104, USA. <sup>2</sup>Department of Statistics, Purdue University, West Lafayette, IN 47907, USA. <sup>3</sup>Department of Radiology, University of North Carolina at Chapel Hill, Chapel Hill, NC 27599, USA. <sup>4</sup>Biomedical Research Imaging Center, School of Medicine, University of North Carolina at Chapel Hill, Chapel Hill, NC 27599, USA. <sup>5</sup>Department of Biostatistics, University of North Carolina at Chapel Hill, Chapel Hill, NC 27599, USA. <sup>6</sup>Department of Computer Science, Purdue University, West Lafayette, IN 47907, USA. <sup>7</sup>Department of Genetics, University of North Carolina at Chapel Hill, Chapel Hill, NC 27599, USA. <sup>8</sup>UNC Neuroscience Center, University of North Carolina at Chapel Hill, Chapel Hill, NC 27599, USA. <sup>9</sup>Department of Computer Science, University of North Carolina at Chapel Hill, Chapel Hill, NC 27599, USA. <sup>10</sup>Department of Statistics and Operations Research, University of North Carolina at Chapel Hill, Chapel Hill, NC 27599, USA.

\*Corresponding author. Email: htzhu@email.unc.edu

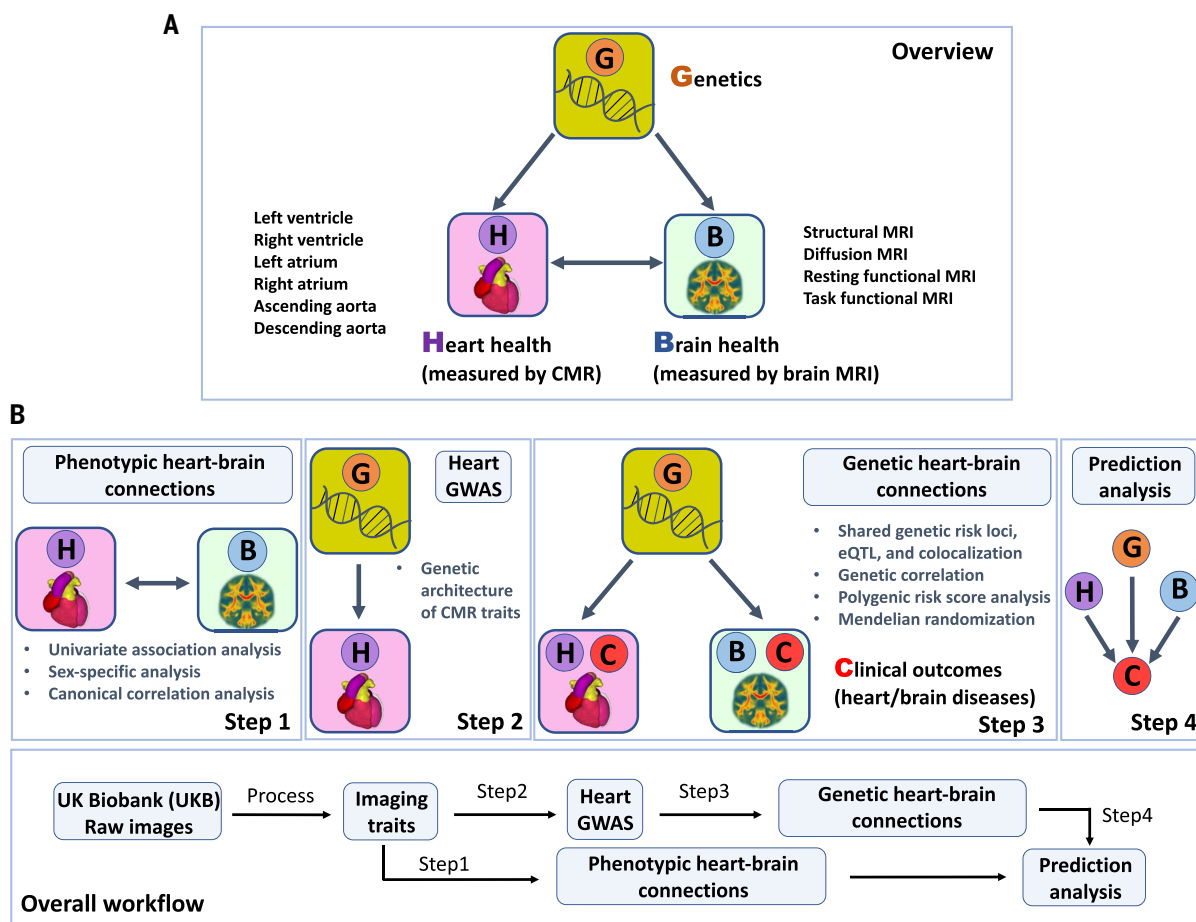


**Fig. 1. Overview of the study design and analyses.** (A) Overview of the study. We used CMR and brain MRI traits as endophenotypes to explore the phenotypic and genetic connections between the heart and the brain. (B) Description of the overall workflow and the key analyses involved in each step.

Some volumetric traits had very high ICC ( $>0.9$ ), including the LV end-diastolic volume (LVEDV), LVM, RV end-diastolic volume (RVEDV), RV end-systolic volume (RVESV), AAo maximum area, AAo minimum area, DAO maximum area, DAO minimum area, and global myocardial wall thickness. The ejection fraction [such as the LV ejection fraction (LVEF)] and distensibility traits (e.g., the DAO distensibility) had the lowest ICC among all volumetric traits (mean = 0.574 and 0.519, respectively). In addition, the average ICC was 0.760 for the 17 wall thickness traits, 0.532 for the seven longitudinal peak strains, 0.569 for the 17 circumferential strains, and 0.516 for the 17 radial strains. Additionally, we examined the changes in 82 CMR traits over a 2-year period and were able to replicate the direction of most of the aging effects (per 7.5 years) described in (55) [table S1 and supplementary text (59)]. Overall, these results suggest that the extracted CMR traits have moderate to high within-subject reliability and can consistently delineate the cardiac and aortic structure and function.

We examined the associations between CMR traits and brain MRI traits in UKB individuals of white British ancestry ( $n = 31,152$ ; see the

materials and methods for a list of adjusted covariates). At the Bonferroni significance level ( $P < 1.33 \times 10^{-6}$ ), CMR traits were associated with a wide variety of brain MRI traits, including regional brain volumes, cortical thickness, DTI parameters, and resting and task fMRI traits (Fig. 2A, fig. S2, and table S3). Among the 4193 Bonferroni-significant associations in our discovery sample, 1574 were significant at the nominal level (0.05) in a holdout independent validation dataset ( $n = 5316$ ) with concordant association signs (figs. S3 to S5). For example, global wall thickness was positively associated with the volumes of multiple subcortical brain structures (fig. S2B). Particularly, both left and right putamen volumes were associated with at least 10 wall thickness traits (fig. S4). Subcortical regions across both brain hemispheres showed consistent association patterns, potentially highlighting the robustness of these correlations. Additional examples of replicated associations can be found in the supplementary text (59).

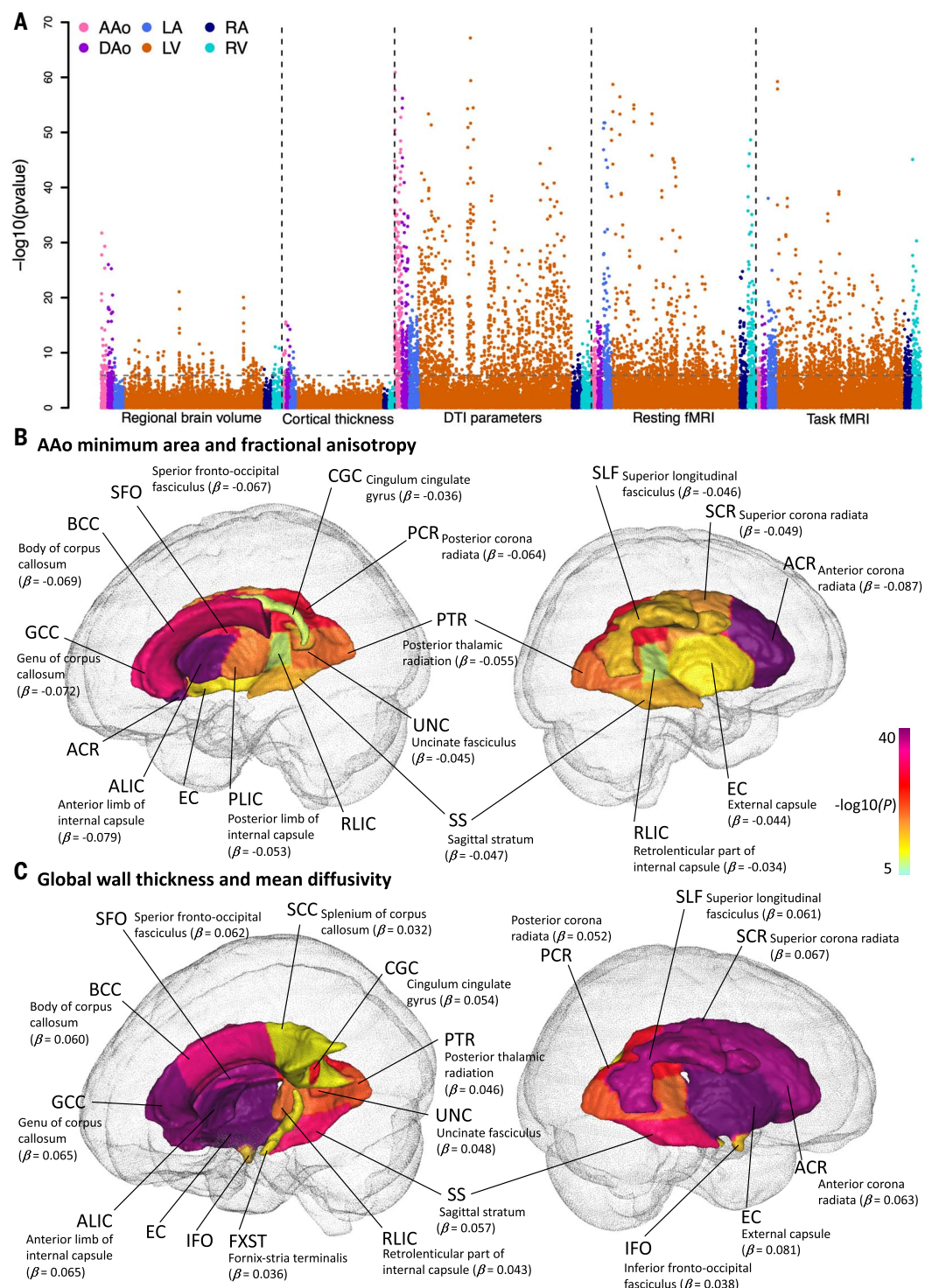
CMR traits were also correlated with brain structural and functional connectivity. For example, fractional anisotropy (FA) and mean diffusivity (MD) are two robust measures of

brain structural connectivity and white matter microstructure, with higher FA and lower MD values typically signifying better white matter integrity (65). The FA values of several white matter tracts consistently showed negative associations with aortic areas (e.g., AAo and DAO minimum areas), LV traits (e.g., LVM, LVEDV, and wall thickness traits), and LA minimum volume ( $LAV_{min}$ ). Moreover, these CMR traits exhibited consistent positive associations with MD values (Fig. 2, B and C, and fig. S6). For resting fMRI, both mean functional connectivity and mean amplitude (i.e., functional activity) traits were negatively associated with volumetric measures of the four cardiac chambers, such as the LV cardiac output (LVCO), RV ejection fraction (RVEF), LA stroke volume (LASV), and RA ejection fraction (RAEF) (fig. S7). By contrast, positive correlations were widely observed for wall thickness traits, longitudinal strains, and peak circumferential strains. The task fMRI traits showed similar patterns (fig. S8). To further discover fine-grained details of CMR connections with brain functions, we examined pairwise associations between 82 CMR traits and 64,620 high-resolution functional connectivity traits (49) in resting fMRI.

**Fig. 2. Phenotypic heart-brain associations.**

(A) The  $-\log_{10}(P)$  value of phenotypic correlations between 82 CMR traits and five groups of brain MRI traits, including 101 regional brain volumes, 63 cortical thickness traits, 110 DTI parameters, 92 resting fMRI traits, and 92 task fMRI traits. The dashed line indicates the Bonferroni significance level ( $P < 1.33 \times 10^{-6}$ ). Each CMR trait category is labeled with a different color.

(B) Significant correlations ( $P < 1.33 \times 10^{-6}$ ) between fractional anisotropy values of white matter tracts and AAo minimum area. (C) Significant correlations ( $P < 1.33 \times 10^{-6}$ ) between mean diffusivity values of white matter tracts and global myocardial wall thickness at end diastole (global wall thickness).



Bonferroni-significant associations ( $P < 7.15 \times 10^{-8}$ ) were observed across the functional connectivity of the whole brain, with specific patterns emerging across different functional areas and networks (fig. S9, A and B). For example, the somatomotor network and its connectivity with the secondary visual network were associated with multiple CMR traits. Specifically, positive somatomotor associations were ob-

served in the LVM, RVEF, RA minimum volume ( $RAV_{min}$ ), global peak circumferential strain, and global wall thickness (figs. S9C and S10 to S13), and negative correlations were observed in all four ejection fraction traits [RVEF, LA ejection fraction (LAEF), RAEF, and LVEF] and LVCO (figs. S9D and S14 to S17). Additional examples can be found in the supplementary text (59) (figs. S18 to S28). Furthermore, we performed the

above phenotypic association analyses separately for males and females (figs. S29 to S32), used canonical correlation analysis (CCA) (66) to investigate the multivariate associations between CMR traits and various groups of brain MRI traits, and examined the influence of environmental factors and biomarkers on the underlying mechanisms of heart-brain interactions [figs. S33 to S35, table S4, and supplementary text (59)].

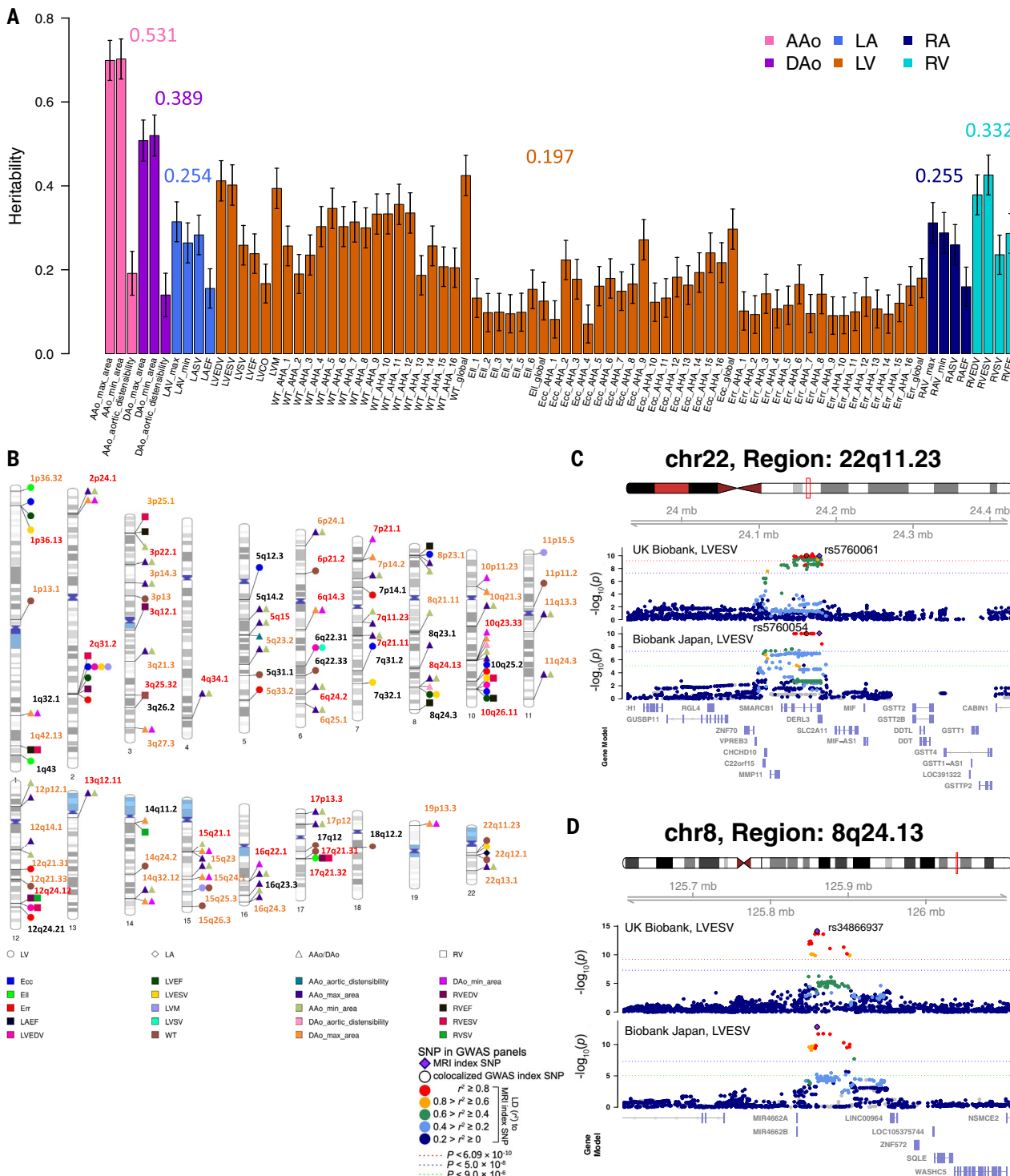


**Fig. 3. Genetics of CMR traits in the UKB.** **(A)** SNP heritability of 82 CMR traits across the six categories. The x axis displays the short names of CMR traits; see table S1 for the full names of these traits. The average heritability of each category is labeled. **(B)** Ideogram of 80 genomic regions associated with CMR traits ( $P < 6.09 \times 10^{-10}$ ). Red and brown name labels denote genomic regions that have been replicated in the validation dataset after applying Bonferroni correction and at a nominal level, respectively. **(C)** LVESV was associated with the 22q11.23 region in both the UKB (index variant rs5760061) and BBJ (index variant rs5760054) studies. **(D)** LVESV was associated with the 8q24.13 region in both the UKB and BBJ studies (shared index variant rs34866937).

## **Heritability and the associated genetic loci of 82 CMR traits**

We estimated the single-nucleotide polymorphism (SNP) heritability for the 82 CMR traits using UKB individuals of white British ancestry.

try (67) ( $n = 31,875$ ). The mean heritability ( $h^2$ ) was 22.9% for the 82 traits (range = 7.07 to 70.2%; Fig. 3A), all of which remained significant after adjusting for multiple testing using the Benjamini-Hochberg procedure to control

the false discovery rate (FDR) at the 0.05 level ( $P < 1.09 \times 10^{-3}$ ) (table S5). The  $h^2$  of the AAo/DAO maximum areas and AAo/DAO minimum areas was >50%. Among cardiac traits, the global wall thickness, RVESV, RVEDV, LV end-systolic

volume (LVESV), LVEDV, and LVM had the highest heritability ( $h^2 > 37.8\%$ ). A sex-specific heritability analysis was conducted separately for females and males, and the heritability estimates for both sexes were similar (mean  $h^2 = 24.8$  versus 22.6%, correlation = 0.910,  $P = 0.332$ ; fig. S36).

We next performed GWASs for the 82 CMR traits using this white British cohort ( $n = 31,875$ ). All Manhattan and QQ plots can be browsed through the server on Heart-KP. The intercepts of linkage disequilibrium (LD) score regression (LDSC) (68) were all close to one, suggesting no genomic inflation of test statistics caused by confounding factors (mean intercept = 0.99986; range = 0.982 to 1.019). At the significance level  $6.09 \times 10^{-10}$  ( $5 \times 10^{-8}/82$ ), that is, the standard GWAS significance threshold, additionally Bonferroni adjusted for the 82 traits), we identified independent (LD  $r^2 < 0.1$ ) significant associations in 80 genomic regions (cytogenetic bands) for 49 CMR traits, including 35 for LV, 35 for AAo, 14 for DAo, 11 for RV, and 1 for LA (Fig. 3B and table S6). Detailed interpretations of these identified regions can be found below. These genetic effects on CMR traits were highly consistent in the sex-specific GWASs, in which males and females were analyzed separately (correlation = 0.944;  $P = 0.739$ ; fig. S37). In the supplementary text (59), we further demonstrate that these CMR traits exhibited a highly polygenic genetic architecture and shared heritability with brain MRI traits, particularly with DTI parameters measuring white matter microstructure (figs. S38 and S39 and table S7).

To replicate the identified loci, we performed separate GWASs using holdout datasets in the UKB study that were independent from our discovery dataset. First, we repeated GWASs on a European dataset with 8252 subjects (see the materials and methods). For the 243 independent (LD  $r^2 < 0.1$ ) CMR-variant associations in the 80 genomic regions, 56 (23.04%, in 25 regions) passed the Bonferroni significance level ( $2.06 \times 10^{-4}$ , 0.05/243) in this European validation GWAS, and 178 (73.25%, in 61 regions) passed the nominal significance level (0.05) (Fig. 3B and table S8). All 178 associations had concordant directions in the two independent GWASs, and the correlation of their genetic effects was 0.963 (fig. S40). These results show a high degree of generalizability of our GWAS findings among European cohorts. We also performed GWAS on two non-European UKB validation datasets: the UKB Asian (UKBA,  $n = 500$ ) and UKB Black (UKBBL,  $n = 271$ ). One association between 8q24.3 and the RVEF passed the Bonferroni significance level ( $P = 8.281 \times 10^{-5}$ ) in UKBA, and 14 more regions passed the nominal significance level. For UKBBL, 12 regions passed the nominal significance level, and none of them survived the Bonferroni significance level, which may

be partially caused by the small sample size of this non-European GWAS. Additionally, we evaluated the ancestry-specific effects using Asian GWAS summary statistics of three CMR traits [analogous to the LVEDV, LVESV, and LVEF (41)], which were generated from 19,000 subjects in the BioBank Japan (BBJ) study (69). At the stringent GWAS  $1.666 \times 10^{-8}$  ( $5 \times 10^{-8}/3$ ) threshold, BBJ CMR traits identified independent (LD  $r^2 < 0.1$ ) significant associations in 22q11.23, 8q24.13, and 10q22.2. Of the three regions, 22q11.23 and 8q24.13 were among the 80 regions that were discovered in the UKB white British cohort. These two regions were significantly associated with the LVSEV in both the UKB and the BBJ studies (Fig. 3, C and D). The 10q22.2 had a small  $P$  value in the UKB GWAS ( $P = 1.58 \times 10^{-9}$ ), but did not survive the  $6.09 \times 10^{-10}$  threshold.

Finally, we constructed polygenic risk scores (PRSs) using lassosum (70) to evaluate the out-of-sample prediction power of the discovery GWAS results (see the materials and methods). Among the 82 CMR traits, 75 had significant PRS at the FDR 5% level ( $P$  range =  $4.47 \times 10^{-125}$  to  $3.74 \times 10^{-2}$ ; table S9). The highest incremental  $R^2$  value (after adjusting for the effects of covariates) was observed on the AAo minimum area and the AAo maximum area (7.20 and 7.04%, respectively). To evaluate the cross-population performance, PRS was also constructed on UKB white British discovery GWAS data using BBJ GWAS summary statistics of the LVEDV, LVESV, and LVEF. We found that the PRSs of these three traits were all significant in the UKB ( $P$  range =  $1.58 \times 10^{-11}$  to  $8.13 \times 10^{-7}$ ;  $R^2$  range =  $3.90 \times 10^{-4}$  to  $1.35 \times 10^{-3}$ ). The prediction accuracy was lower than that in the above within European prediction analysis ( $R^2$  range =  $7.72 \times 10^{-3}$  to  $9.67 \times 10^{-3}$ ), which may be explained by the smaller training GWAS sample size in the BBJ study and population differences between the UKB and BBJ cohorts.

### Pleiotropy of genetic variants across body systems

To identify the shared genetic effects between CMR traits and complex traits, we performed association lookups for independent (LD  $r^2 < 0.1$ ) significant variants (and variants in their LD,  $r^2 \geq 0.6$ ,  $P < 6.09 \times 10^{-10}$ ) detected in our UKB white British GWAS. In the National Human Genome Research Institute–European Bioinformatics Institute (NHGRI-EBI) GWAS catalog (71), our results tagged variants that have been linked to a wide range of traits and diseases, including heart diseases, heart structure and function, blood pressure, lipid traits, blood traits, diabetes, stroke, neurological and neuropsychiatric disorders, psychological traits, cognitive traits, lung function, parental longevity, smoking, and drinking. To evaluate whether two associated genetic signals were consistent with the shared causal variant, we

applied the Bayesian colocalization analysis (72) for CMR traits and selected phenotypes with publicly available GWAS summary statistics. Evidence of pairwise colocalization was defined as having a posterior probability of the shared causal variant hypothesis (PPH4) > 0.8 (72, 73). Many shared genetic variants were found to be expression quantitative trait loci (eQTLs) in a recent large-scale eQTL meta-analysis of brain (74) and blood tissues (75). The traits with shared genetic effects are presented in table S10, with selected pairs shown in Fig. 4 and figs. S41 to S108. Table S11 summarizes the results of colocalization and eQTL analyses. Below, we highlight genetic overlaps between CMR traits and complex traits and diseases of the heart and brain, as well as other clinical outcomes.

First, we replicated 27 genomic regions that have been previously linked to cardiac and aortic traits, such as fractional shortening and LV internal dimension (fig. S41). There were 21 regions associated with heart rate and electrocardiographic traits (e.g., QRS duration; figs. S42 to S46) and six regions with aortic measures (e.g., thoracic aortic aneurysms and dissections; figs. S47 and S48). In addition, 30 regions had shared associations (LD  $r^2 \geq 0.6$ ) with cardiovascular diseases, including 12 regions with coronary artery disease (76) (figs. S49 and S50), nine regions with atrial fibrillation (77) (Fig. 4A and figs. S51 to S55), and five regions with hypertension (78) (figs. S56 to S58). Other heart diseases included abdominal aortic aneurysm (79) (figs. S47 and S59), mitral valve prolapse (80) (fig. S46), and idiopathic dilated cardiomyopathy (81) (figs. S60 and S61). There was widespread evidence of colocalization on many loci (PPH4 > 0.899). Additionally, 41 of the 80 genomic regions were associated with blood pressure traits such as diastolic or systolic blood pressure, pulse pressure, and mean arterial pressure (Fig. 4B and figs. S62 to S81). CMR traits were in LD ( $r^2 \geq 0.6$ ) with various cardiovascular and blood biochemistry biomarkers such as lipid traits (figs. S50, S56, S67, and S82), red blood cell count, blood protein levels, red cell distribution width, and plateletcrit (figs. S83 to S87).

We found genetic pleiotropy between CMR traits and multiple brain-related complex traits and disorders. In the 6p21.2, 7p21.1, and 12q24.12 regions, CMR traits were in LD ( $r^2 \geq 0.6$ ) with stroke (82) (e.g., ischemic stroke, large artery stroke, and small-vessel ischemic stroke), intracranial aneurysm (83), and moyamoya disease (84) (Fig. 4, A and B, and fig. S50). The index variants of 7p21.1 (rs2107595) and 12q24.12 (rs597808) were eQTLs of *TWIST1* and *ALDH2* in human brain tissues (74), suggesting that these CMR-associated variants were known to affect gene expression in human brain. *TWIST1* was associated with cerebral vasculature defects (85), and there was a higher level of *ALDH2*

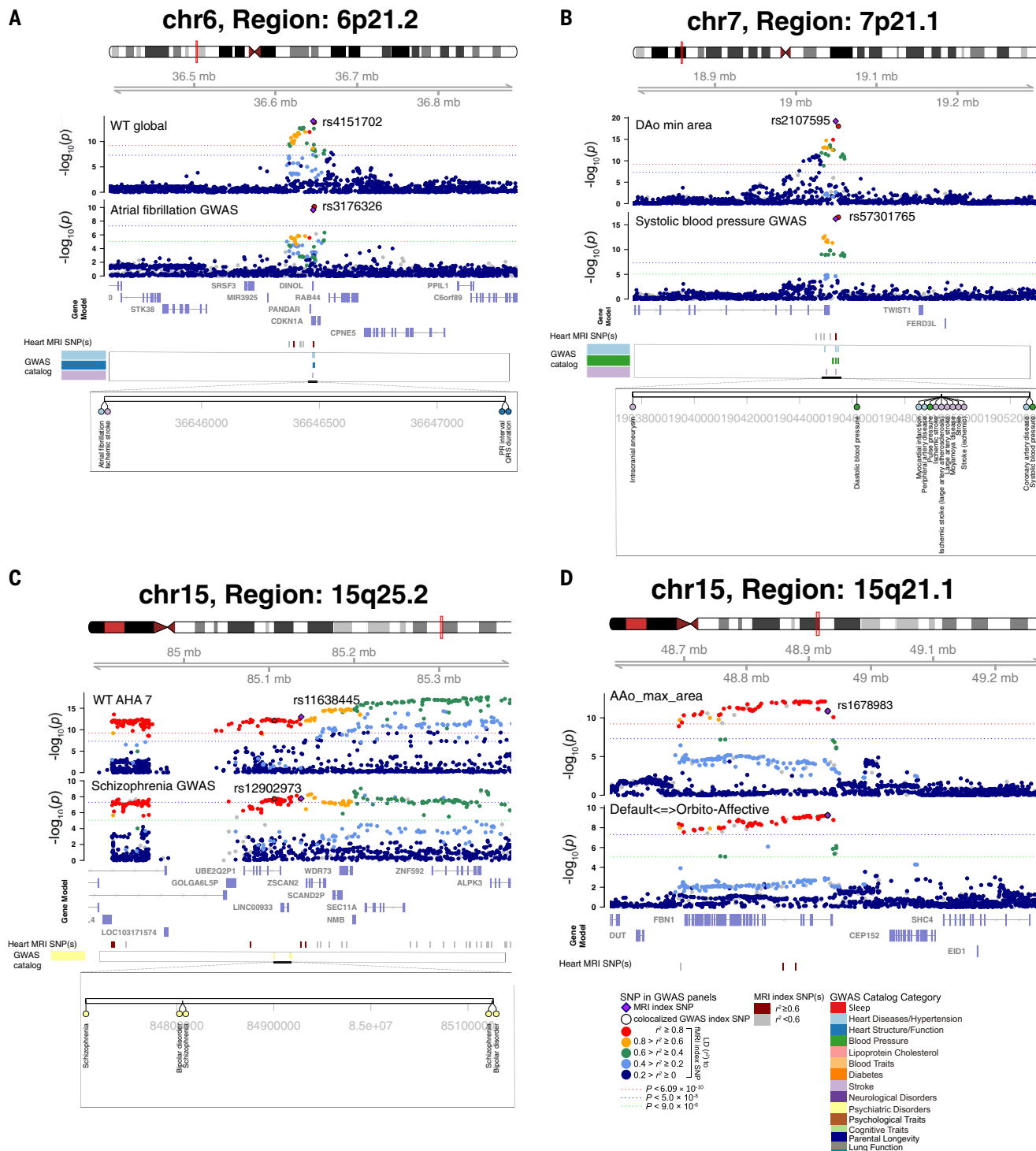


**Fig. 4. Selected genetic loci associated with both CMR trait and other complex traits and diseases.** (A) In 6p21.2, we observed colocalization between the global myocardial wall thickness (WT) at end-diastole (WT global, index variant rs4151702) and atrial fibrillation (index variant rs3176326). The posterior probability of Bayesian colocalization analysis for the shared causal variant hypothesis (PPH4) is 0.997. In this region, the WT global was also in LD ( $r^2 \geq 0.6$ ) with ischemic stroke. (B) In 7p21.1, we observed colocalization between the DAO minimum area (DAO min area, index variant rs2107595) and systolic blood pressure (index variant rs57301765, PPH4 = 0.998). In this region, the DAO min area was also in LD with stroke, intracranial aneurysm, coronary artery disease, and moyamoya disease. (C) In 15q25.2, we observed colocalization between the regional myocardial wall thickness at end-diastole (WT AHA 7, index variant rs11638445) and schizophrenia (index variant rs12902973, PPH4 = 0.922). In this region, the WT AHA 7 was also in LD with bipolar disorder. AHA 7, American Heart Association (AHA) region 7. (D) We illustrated the colocalization between the AAo maximum area (AAo max area) and functional connectivity between the default mode and orbito-affective networks (shared index variant rs1678983) in 15q21.1 (PPH4 = 0.964).

activity in the putamen and temporal cortex of patients with Alzheimer's disease (86). CMR traits were also in LD ( $r^2 \geq 0.6$ ) with neurodegenerative and neuropsychiatric disorders such as Parkinson's disease (87) and Alzheimer's disease (88) (fig. S88), hippocampal sclerosis of aging (89) (fig. S74), schizophrenia (90) (Fig. 4C and fig. S49), bipolar disorder (91) (Fig. 4C and figs. S82 and S89), and eating disorders (92) (fig. S90). In addition, CMR traits were in LD ( $r^2 \geq 0.6$ ) with mental health traits such as neuroticism, depressive symptoms, subjective well-being, and risk-taking tendency (figs. S88 and S91 to S93).

For cognitive traits and education, we tagged 17q21.31, 11p11.2, and 11q13.3 with cognitive function and educational attainment (figs. S88, S93, and S94); 7q32.1 with reading disability (fig. S95); and 12q24.12 with reaction time (fig. S50). We also found shared associations (LD  $r^2 \geq 0.6$ ) in five regions with DTI parameters (47) (figs. S96 to S100); four regions with regional brain volumes (45) (figs. S101 to S104); and five regions with fMRI traits (49) (Fig. 4D and figs. S105 to S108). The colocalization analysis revealed that CMR traits shared causal genetic variants with these phenotypes, such as 15q25.2 with schizophrenia, 15q21.1 with functional connectivity, as well as 11q24.3 and 12q24.12 with white matter microstructure (PPH4  $> 0.809$ ). There is substantial evidence supporting the interplay between cardiovascular health and these brain traits and diseases. For example, people with better heart health have better cognitive abilities (93) and lower risk for brain disorders such as stroke and Alzheimer's disease (94). In addition, mental health disorders may result in biological processes and behaviors that are associated with cardiovascular diseases (11, 95). Our findings indicate that cardiovascular conditions share substantial genetic components with brain diseases, mental health traits, and cognitive functions, suggesting a potential genetic basis for heart-brain connections.

Genetic overlaps with other diseases and complex traits were also observed. For example, RVEDV was in LD ( $r^2 \geq 0.6$ ) with type 1 diabetes (96) and type 2 diabetes (97, 98) in the 12q24.12 region (fig. S50). CMR traits were in LD ( $r^2 \geq 0.6$ ) in 11 regions with lung conditions such as asthma (99) (fig. S82), idiopathic pulmonary fibrosis (100), interstitial lung disease (101) (fig. S88), and lung function (figs. S60, S64, S67, and S77). We also found shared genetic associations (LD  $r^2 \geq 0.6$ ) with smoking (figs. S50, S82, and S93) and alcohol consumption and alcohol use disorder (figs. S49, S88, and S93).

#### Genetic correlations with brain disorders and complex traits

First, we examined genetic correlations among 82 CMR traits using cross-trait LDSC (102).

Strong genetic correlations were observed within and between categories of CMR traits (fig. S109 and table S12). For example, RVEDV was genetically correlated with other RV traits, including RV stroke volume (RVSV), RVESV, and RVEF. The RVEDV was also correlated with CMR traits from other categories, such as AAo maximum area and DAo maximum area, LASV and RA stroke volume (RASV), as well as LVEDV, LVESV, LVM, and LVEF. In addition, we found a strong relationship between phenotypic and genetic correlations among all CMR traits ( $\beta = 0.781, P < 2 \times 10^{-16}$ ).

Next, we examined the genetic correlations between 82 CMR traits and 60 complex traits and diseases. At the FDR 5% level (82  $\times$  60 tests), the CMR traits were associated with heart diseases, lung function, cardiovascular risk factors, and brain-related complex traits and diseases (table S12). For example, hypertension had clear genetic correlations with aortic traits and LV traits (Fig. 5A). The strongest correlation between LV traits and hypertension was found in wall thickness traits ( $P < 2.43 \times 10^{-9}$ ), which were also associated with coronary artery disease, type 2 diabetes, and stroke (Fig. 5B). In addition, atrial fibrillation was significantly associated with aortic, LA, and RA traits ( $P < 6.66 \times 10^{-4}$ ), suggesting that atrial fibrillation might have a higher genetic similarity with LA and RA traits than with LV and RV traits.

In both schizophrenia and bipolar disorder, we observed genetic correlations with multiple LV traits (Fig. 5C). Specifically, LVCO, LVEF, radial strains, and wall thickness traits showed positive genetic correlations with schizophrenia and/or bipolar disorder. By contrast, peak circumferential strains had negative genetic correlations with the two brain disorders. Additionally, anorexia nervosa (an eating disorder) was genetically associated with LAV<sub>min</sub> and LAEF, whereas cognitive traits and neuroticism were mainly associated with right heart traits (RA and RV traits) (Fig. 5, D and E). For example, intelligence, cognitive function, and numerical reasoning were genetically correlated with RA volumes. Lung functions (FEV and FVC) had genetic correlations with multiple CMR traits, with longitudinal strains showing the strongest correlations. There were more associations with other complex traits analyzed in previous GWAS, such as smoking, PR interval, blood pressure, education, risky behaviors, and lipid traits (fig. S110A). We also found high genetic correlations with four previously reported LV traits (41) (genetic correlation  $> 0.847, P < 6.44 \times 10^{-201}$ ) (fig. S110B). Additionally, we built PRS for 82 CMR traits and examined their associations with 276 phenotypes available in the UKB study. The PRS analysis produced genetic association patterns similar to those from the LDSC analysis. More details and interpretations are available in the sup-

plementary text (59) (figs. S111 and S112 and table S13).

#### Causal heart-brain relationships detected by Mendelian randomization

In light of the widespread genetic correlations between the heart and brain, we examined their underlying causal genetic links using the 82 CMR traits with Mendelian randomization (MR) (103).

We investigated 11 well-powered ( $n > 20,000$ ) brain-related clinical outcomes from the FinnGen database (104) and six neuropsychiatric disorders from the Psychiatric Genomics Consortium (105). We also evaluated nine cognitive and mental health traits such as intelligence and neuroticism (see the materials and methods).

Most of the MR findings indicated genetic causal effects from the heart to the brain (table S14 and fig. S113). We identified causal genetic links underlying heart health and neuropsychiatric disorders. Specifically, multiple genetic causal effects of wall thickness traits, DAo minimum area, and LVESV to psychiatric diseases and mental health traits were identified at the FDR 5% level ( $P < 1.68 \times 10^{-4}$ ), such as the cross disorders [five major psychiatric disorders (106)], bipolar disorder, and depression (Fig. 6). The presence of heart conditions may adversely affect attitude and mood, which may ultimately lead to mental health problems such as depression and other psychiatric disorders (107). For example, hypertrophic cardiomyopathy is associated with an increased risk of mood disorders (108). Heart muscle thickening makes it more difficult for the heart to pump blood, and when oxygen to the brain is reduced, mental health issues may develop (109). We also observed causal genetic effects of wall thickness traits on neuroticism, for which the phenotypic association has been identified (55). Moreover, AAo minimum area and AAo maximum area were causally linked to multiple FinnGen diseases of the nervous system, such as neurological diseases, sleep apnea, and episodic and paroxysmal disorders. Conversely, we identified several causal relationships in which brain disorders were the exposure and CMR traits were the outcome; most of these were from sleep apnea to radial strains. In previous studies, the reduction in radial strain has been found in patients with moderate to severe obstructive sleep apnea (110), and our results demonstrate that this association may have a causal genetic component.

#### Biological and gene-level analyses

We performed gene-level association testing using GWAS summary statistics of the 82 CMR traits with MAGMA (111). We identified 163 significant genes for 48 CMR traits ( $P < 3.24 \times 10^{-8}$ , Bonferroni adjusted for 82 traits) (table S15). Next, we mapped significant variants ( $P < 6.09 \times 10^{-10}$ ) to genes by combining evidence

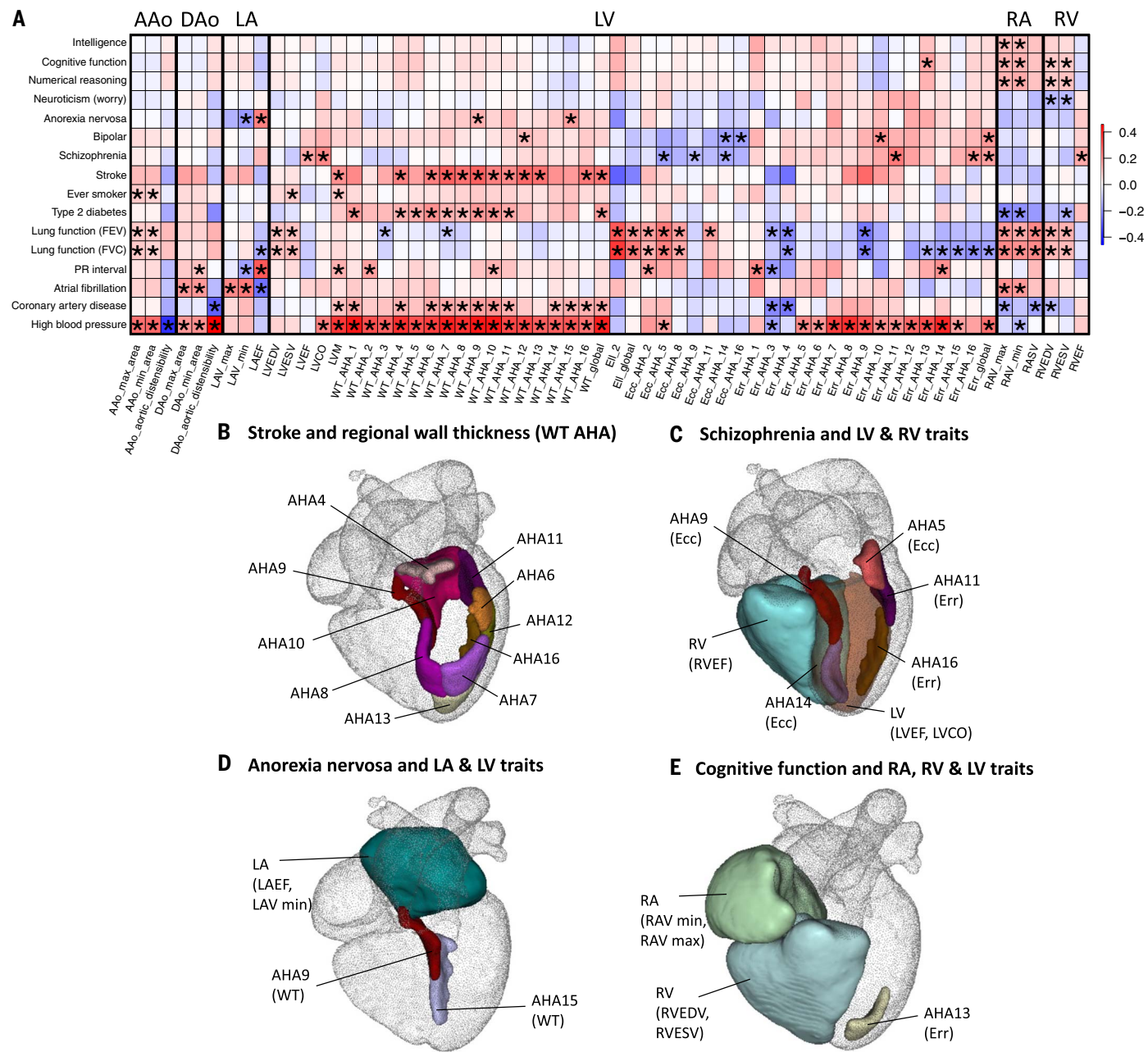


**Fig. 5. Genetic correlations between CMR traits and other complex traits and diseases.** (A) We illustrated selected genetic correlations between CMR traits (x axis) and complex traits and diseases (y axis). The asterisks highlight genetic correlations that have passed multiple testing adjustments using the Benjamini-Hochberg procedure to control the FDR at the 5% level. (B to E) Illustration of CMR traits that exhibited genetic correlations with stroke (B), schizophrenia (C), anorexia nervosa (D), and cognitive function (E).

of physical position, eQTL association, and three-dimensional chromatin (Hi-C) interaction using FUMA (112). We found 585 mapped genes, 440 of which were not identified in MAGMA (table S16). Moreover, 91 MAGMA or FUMA-identified genes had a high probability of being loss-of-function intolerant (113) ( $pLI > 0.98$ ), indicating significant enrichment of intolerance of loss-of-function variation among these CMR-associated genes ( $P = 1.68 \times 10^{-4}$ ). We conducted MAGMA gene-set analysis to prioritize enriched biological pathways and

performed partitioned heritability analyses (114) to identify tissues and cell types (115) in which genetic variation contributed to differences in CMR traits [fig. S114, table S17, and supplementary text (59)].

Ten genes were targets for 32 cardiovascular system drugs (116), such as 15 calcium channel blockers [anatomical therapeutic chemical (ATC) code: C08] to lower blood pressure, five cardiac glycosides (ATC code: C01A) to treat heart failure and irregular heartbeats, and three antiarrhythmics (ATC code: C01B) to

treat heart rhythm disorders (table S18). Three of these genes, *C4NAII*, *ESRI*, and *CYP2C9*, and four more CMR-associated genes, *ALDH2*, *HDAC9*, *NPSR1*, and *TRPA1*, were targets for 11 nervous system drugs, including four anti-epileptic drugs (ATC code: N03A) and two drugs for addictive disorders (ATC code: N07B). Some drug target genes have known biological functions in both the heart and the brain. For example, *ALDH2* plays a role in clearance of toxic aldehydes, which is an important mechanism related to myocardial and cerebral

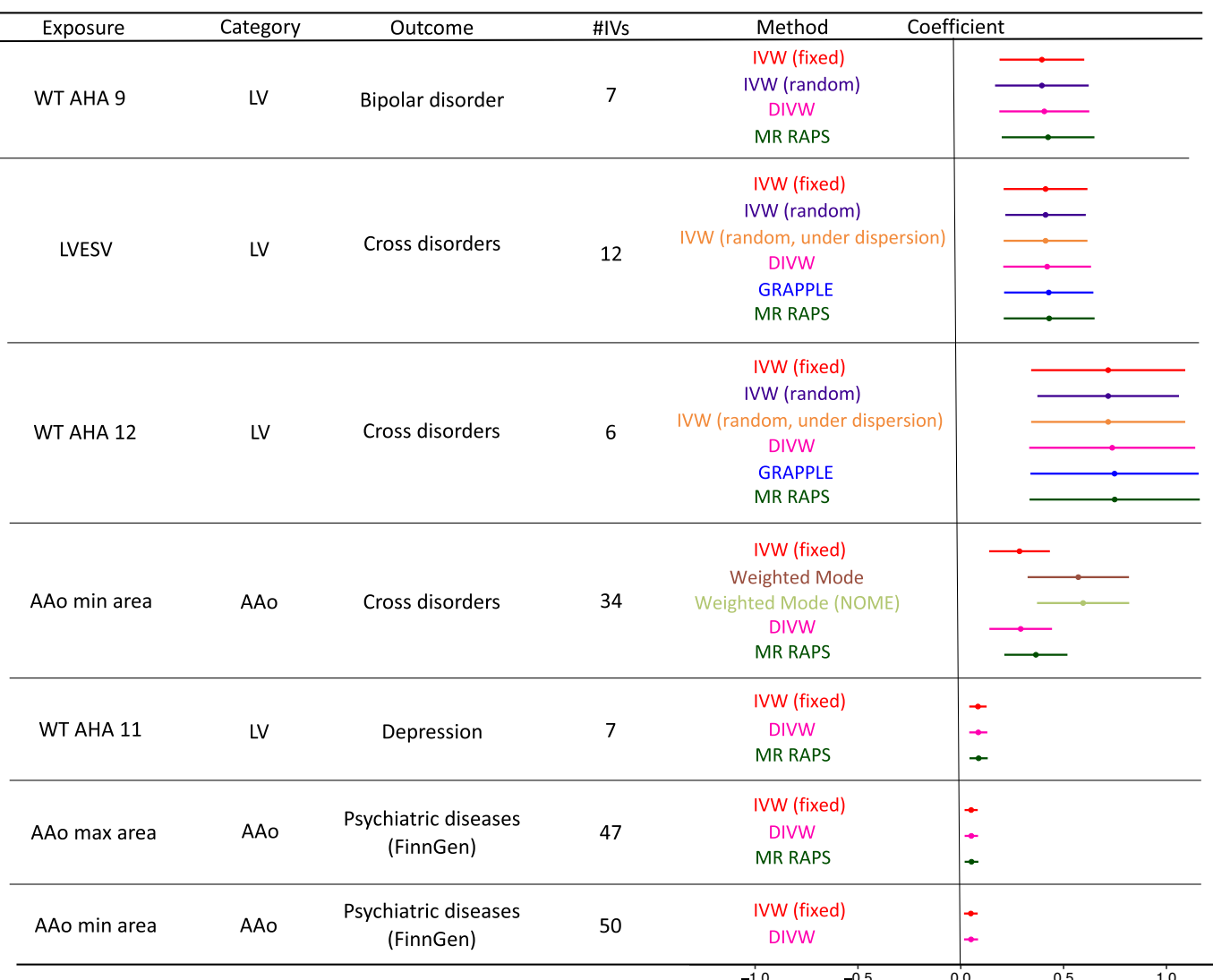


**Fig. 6. Genetic causal effects of CMR traits on psychiatric disorders.** We illustrated selected significant ( $P < 1.68 \times 10^{-4}$ ) causal genetic links from CMR traits (exposure) to psychiatric disorders (outcome) after adjusting for multiple testing using the Benjamini-Hochberg procedure to control the FDR at the 5% level. Category, the category of CMR traits; #IVs, the number of genetic variants used as instrumental variables. Different Mendelian randomization methods and their regression coefficients are labeled with different colors. See table S14 for data resources of psychiatric disorders.

ischemia–reperfusion injury (117). Therefore, *ALDH2* has been proposed to be a protective target for heart and brain diseases and dysfunctions triggered by ischemic injury and related risk factors (118, 119).

Finally, we conducted complex trait and disease prediction using both genetic and multi-organ MRI data. We found that integrating genetic PRS, CMR traits, and brain MRI traits could enhance the prediction of multisystem diseases (e.g., diabetes) compared with using only one data type [figs. S15 and 116, tables S19 and S20, and supplementary text (59)].

## Discussion

The intertwined connections between heart and brain health are gaining increasing attention. This study quantified the heart-brain

associations using CMR and brain MRI data from >40,000 individuals in one study cohort (UKB). After accounting for various body measurements, shared risk factors, and imaging confounders, we discovered that CMR traits were associated with specific brain regions, white matter tracts, and functional networks. For example, LV traits and aortic areas were connected to white matter microstructure, with FA and MD values exhibiting opposite directions. Univariate analysis and CCA indicated that aortic traits were associated with basal forebrain volumes in both the left and right hemispheres. The basal forebrain cholinergic system, which is the primary cholinergic output of the central nervous system, is crucial in cognitive decline and dementia (120, 121). Reduced basal forebrain volume

and vascular dysregulation are early predictors of Alzheimer's disease pathology (122, 123). Moreover, several CMR traits, including LVM and ejection fraction measures, were associated with the somatomotor, auditory, and default mode networks in resting fMRI. The CMR associations with the default mode and other networks were generally in opposite directions. Increased LVM and reduced ejection fraction traits are associated with a higher risk of cardiac diseases (55). Our findings suggest that abnormal functional connectivity within these networks could potentially act as an early biomarker of brain dysfunction associated with adverse cardiac conditions. Overall, our research indicates that there are associations between multimodal MRI measurements of the heart and brain, hinting at

potential connections between cardiovascular and neurological health.

We used multiorgan imaging data to identify genetic variations that can affect both the heart and brain. Comprehending the genetic pleiotropies and the intricate directional and bidirectional interactions of human organs is a complex task (11). Our study provides evidence of causal genetic effects between CMR traits and brain disorders through MR analysis. Because CMR traits are endophenotypes of various cardiovascular diseases (e.g., hypertension and hypertensive diseases), these findings suggest that early intervention in heart conditions and the management of cardiac risk may have a positive impact on brain health. Numerous studies have examined the cognitive and neuropsychiatric effects of anti-hypertensive medications, such as  $\beta$ -blockers and calcium channel blockers (124, 125), and some recent studies reported their beneficial effects on psychiatric and neurological disorders. For example, in a meta-analysis of 209 studies, antihypertensive medications were found to reduce dementia risk by 21% (126). Brain-penetrant calcium channel blockers were associated with a lower incidence of neuropsychiatric disorders (127). The CMR and brain MRI traits prioritized in our heart-brain analyses could be helpful in identifying potential therapeutic targets and evaluating the therapeutic potential (or side effects) of existing antihypertensive drugs and heart disease medications for mental health and neurodegenerative disorders.

To mitigate the confounding effects of body size, our analyses have adjusted for a wide range of variables collected by the UKB study, including height, weight, whole-body fat free mass, waist-to-hip ratio, body surface area, and nonlinear high-order terms (128). However, unobserved biological interactions and environmental factors may still confound the identified heart-brain connections. The concept of large-scale multiorgan imaging genetics analysis is relatively new, and future research using additional data resources, such as long-term longitudinal data and large-scale omics data from multiple organs, may provide further insights into the shared biology between the brain and heart. In addition, our analyses faced challenges because of the use of different brain MRI traits generated from multiple imaging modalities. For example, previous studies have shown that lower FA and higher MD of white matter are associated with accelerated brain aging, indicating reduced microstructural coherence with aging (129). Resting functional connectivity strength has also been often found to be lower in the aging brain (130). In our analyses, certain CMR traits correlated with distinct categories of brain MRI traits in contrasting directions. For example, higher wall thick-

ness was linked to larger subcortical regional brain volumes in structural MRI, lower FA in diffusion MRI, and mostly stronger functional connectivity strength in resting fMRI of cortical brain areas. These findings may suggest that white matter and gray matter are differentially associated with certain heart functions. However, potential confounding factors cannot be completely ruled out, because the MRI traits were from different areas of the brain and extracted using different brain maps and processing procedures. To better establish and investigate these patterns, future studies could incorporate new brain MRI traits, such as microstructure measures in gray matter brain regions, and produce diffusion MRI and fMRI traits in the same brain atlas, allowing for a more comprehensive analysis of the structural and functional relationships between the heart and the brain.

In this study, imaging data were mainly from individuals of European ancestry. Comparing UKB GWAS results with those of BBJ, we found both similarities and differences for genetic influences on CMR traits. For example, participants in UKB and BBJ had similar genetic effects on cardiac conditions at 22q11.23 and 8q24.13, but only the BBJ cohort showed genetic effects at 10q22.2. There was also a reduction in PRS performance in the BBJ-UKB prediction compared with the prediction analysis within the UKB study. Furthermore, the UKB study is well known for its “healthy volunteer” selection bias and may not be an ideal representation of the general European population (131). It can be expected that some of the genetic components that underlie heart-brain connections may be population specific or UKB specific. More open and large-scale imaging datasets (132) collected from global populations may help to identify causal variants associated with CMR traits in globally diverse populations and quantify population-specific heterogeneity of genetic effects. These new data will also enable the development of a better picture of neurological-cardiac interactions and allow researchers to examine the reproducibility of scientific findings.

This paper specifically focuses on heart-brain connections. Because of the large amount of data collected in the UKB study, it is also possible to study the relationships between the brain and other human organs and systems (133). For example, increasing evidence supports the gut-brain axis, which involves complex interactions between the central nervous system and the enteric nervous system (134). Patients with inflammatory bowel disease (e.g., Crohn’s disease) show a higher risk of mental disorders such as depression and anxiety (135). Multisystem analysis using biobank-scale data may provide insights for interorgan pathophysiological mechanisms and guide the prevention and early detection of brain diseases.

## Methods summary

Our study aimed to explore the connection between the heart and brain by analyzing multiorgan imaging data obtained from >40,000 subjects. We used recently developed pipelines for cardiac and aortic MRI (55–57) to generate imaging traits for four cardiac chambers, LV, LA, RV, and RA, and two aortic sections, AAo and DAo. Moreover, we extracted various imaging traits from multiple brain MRI modalities, including structural MRI (47), diffusion MRI (49), and resting-state and task-based fMRI (51). We then performed phenotypic and genetic analyses on these multiorgan imaging traits to examine the relationship between the heart and brain.

We performed a discovery-replication analysis to assess pairwise phenotypic associations between heart and brain imaging traits while controlling for various covariates such as body size (128), shared risk factors, and imaging confounders. Additionally, we conducted separate univariate analyses of structural and functional connection patterns for both female and male subjects. To better understand the relationship between CMR traits and different brain MRI modalities, we used CCA (66) to examine multivariate associations.

We used data from UKB individuals of British ancestry to estimate the SNP heritability of 82 CMR traits (67) and performed GWAS using linear mixed-effect models implemented in fastGWA (136). To ensure the robustness of our findings, we conducted separate GWASs with independent holdout datasets to replicate the identified loci. We also conducted sex-specific SNP heritability and GWAS analyses to compare the genetic effects on CMR traits between males and females. Additionally, we generated PRS (70) to assess the proportion of variation in CMR traits that could be predicted by genetic variants in European and non-European testing cohorts. To investigate gene-level associations, we used MAGMA (95), and we mapped GWAS signals to genes using functional genomic information in FUMA (38).

We used GWAS results of CMR traits to uncover the genetic overlaps with other complex traits and diseases previously identified in GWASs, including our brain MRI traits and those catalogued in the NHGRI-EBI GWAS database (71). We applied Bayesian colocalization analysis (72) to examine the presence of shared causal genetic variants underlying genetic pleiotropy. Additionally, we used cross-trait LDSC (102) to estimate genome-wide genetic correlations between CMR traits and other complex traits and diseases.

We further investigated genetic associations by examining the relationship between PRS of CMR traits and phenotypes collected in the UKB study. We also used additional data resources, such as FinnGen (104), which provided GWAS results on brain-related clinical

outcomes, to conduct a two-sample MR analysis (103) to investigate the genetic causal relationships between CMR traits and brain disorders. Additionally, we evaluated the predictive ability of CMR traits for complex traits and diseases in the UKB study, and improved prediction accuracy by integrating genetic PRS, CMR traits, and brain MRI traits.

## REFERENCES AND NOTES

- H. Gardener, C. B. Wright, T. Rundek, R. L. Sacco, Brain health and shared risk factors for dementia and stroke. *Nat. Rev. Neurol.* **11**, 651–657 (2015). doi: [10.1038/nrneuro.2015.195](https://doi.org/10.1038/nrneuro.2015.195); pmid: [26481296](https://pubmed.ncbi.nlm.nih.gov/26481296/)
- I. J. Brodatz *et al.*, Dissecting the genetic relationship between cardiovascular risk factors and Alzheimer's disease. *Acta Neuropathol.* **137**, 209–226 (2019). doi: [10.1007/s00401-018-1928-6](https://doi.org/10.1007/s00401-018-1928-6); pmid: [30413934](https://pubmed.ncbi.nlm.nih.gov/30413934/)
- A. Papadopoulos *et al.*, Left ventricular hypertrophy and cerebral small vessel disease: A systematic review and meta-analysis. *J. Stroke* **22**, 206–224 (2020). doi: [10.5853/jos.2019.03335](https://doi.org/10.5853/jos.2019.03335); pmid: [32635685](https://pubmed.ncbi.nlm.nih.gov/32635685/)
- P. Abete *et al.*, Cognitive impairment and cardiovascular diseases in the elderly. A heart-brain continuum hypothesis. *Ageing Res. Rev.* **18**, 41–52 (2014). doi: [10.1016/j.arr.2014.07.003](https://doi.org/10.1016/j.arr.2014.07.003); pmid: [25107566](https://pubmed.ncbi.nlm.nih.gov/25107566/)
- F. Moroni *et al.*, Cardiovascular disease and brain health: Focus on white matter hyperintensities. *Int. J. Cardiol. Heart Vasc.* **19**, 63–69 (2018). doi: [10.1016/j.ijcha.2018.04.006](https://doi.org/10.1016/j.ijcha.2018.04.006); pmid: [29946567](https://pubmed.ncbi.nlm.nih.gov/29946567/)
- C. S. Kwok, Y. K. Loke, R. Hale, J. F. Potter, P. K. Myint, Atrial fibrillation and incidence of dementia: A systematic review and meta-analysis. *Neurology* **76**, 914–922 (2011). doi: [10.1212/WNL.0b013e318202e38](https://doi.org/10.1212/WNL.0b013e318202e38); pmid: [21383328](https://pubmed.ncbi.nlm.nih.gov/21383328/)
- A. Kobayashi, M. Iguchi, S. Shimizu, S. Uchiyama, Silent cerebral infarcts and cerebral white matter lesions in patients with nonvalvular atrial fibrillation. *J. Stroke Cerebrovasc. Dis.* **21**, 310–317 (2012). doi: [10.1016/j.jstrokecerebrovasdis.2010.09.004](https://doi.org/10.1016/j.jstrokecerebrovasdis.2010.09.004); pmid: [2111632](https://pubmed.ncbi.nlm.nih.gov/2111632/)
- D. Kim *et al.*, Risk of dementia in stroke-free patients diagnosed with atrial fibrillation: Data from a population-based cohort. *Eur. Heart J.* **40**, 2313–2323 (2019). doi: [10.1093/euheartj/ehz386](https://doi.org/10.1093/euheartj/ehz386); pmid: [31212315](https://pubmed.ncbi.nlm.nih.gov/31212315/)
- R. L. Vogels, P. Scheltens, J. M. Schroeder-Tanka, H. C. Weinstein, Cognitive impairment in heart failure: A systematic review of the literature. *Eur. J. Heart Fail.* **9**, 440–449 (2007). doi: [10.1016/j.ejheart.2006.11.001](https://doi.org/10.1016/j.ejheart.2006.11.001); pmid: [17174152](https://pubmed.ncbi.nlm.nih.gov/17174152/)
- L. Meng, W. Hou, J. Chui, R. Han, A. W. Gelb, Cardiac output and cerebral blood flow: The integrated regulation of brain perfusion in adult humans. *Anesthesiology* **123**, 1198–1208 (2015). doi: [10.1097/ALN.00000000000000872](https://doi.org/10.1097/ALN.00000000000000872); pmid: [26402848](https://pubmed.ncbi.nlm.nih.gov/26402848/)
- G. N. Levine *et al.*, Psychological health, well-being, and the mind-heart-body connection: A scientific statement from the American Heart Association. *Circulation* **143**, e763–e783 (2021). doi: [10.1161/CIR.0000000000000947](https://doi.org/10.1161/CIR.0000000000000947); pmid: [33486973](https://pubmed.ncbi.nlm.nih.gov/33486973/)
- D. S. Krantz, M. M. Burg, Current perspective on mental stress-induced myocardial ischemia. *Psychosom. Med.* **76**, 168–170 (2014). doi: [10.1097/PSY.0000000000000054](https://doi.org/10.1097/PSY.0000000000000054); pmid: [24677165](https://pubmed.ncbi.nlm.nih.gov/24677165/)
- S. S. Abisse, R. Lampert, M. Burg, R. Soufer, V. Shusterman, Cardiac repolarization instability during psychological stress in patients with ventricular arrhythmias. *J. Electrocardiol.* **44**, 678–683 (2011). doi: [10.1016/j.jelectrocard.2011.07.019](https://doi.org/10.1016/j.jelectrocard.2011.07.019); pmid: [21920534](https://pubmed.ncbi.nlm.nih.gov/21920534/)
- R. Jindal, E. M. MacKenzie, G. B. Baker, V. K. Yeragani, Cardiac risk and schizophrenia. *J. Psychiatry Neurosci.* **30**, 393–395 (2005). pmid: [16327872](https://pubmed.ncbi.nlm.nih.gov/16327872/)
- R. E. Nielsen, J. Banner, S. E. Jensen, Cardiovascular disease in patients with severe mental illness. *Nat. Rev. Cardiol.* **18**, 136–145 (2021). doi: [10.1038/s41569-020-00463-7](https://doi.org/10.1038/s41569-020-00463-7); pmid: [33128044](https://pubmed.ncbi.nlm.nih.gov/33128044/)
- A. Tawakol *et al.*, Relation between resting amygdalar activity and cardiovascular events: A longitudinal and cohort study. *Lancet* **389**, 834–845 (2017). doi: [10.1016/S0140-6736\(16\)31714-7](https://doi.org/10.1016/S0140-6736(16)31714-7); pmid: [28088338](https://pubmed.ncbi.nlm.nih.gov/28088338/)
- R. L. Verrier, T. D. Pang, B. D. Nearing, S. C. Schachter, The Epileptic Heart: Concept and clinical evidence. *Epilepsy Behav.* **105**, 106946 (2020). doi: [10.1016/j.yebeh.2020.106946](https://doi.org/10.1016/j.yebeh.2020.106946); pmid: [32109857](https://pubmed.ncbi.nlm.nih.gov/32109857/)
- J. Hinterdobler *et al.*, Acute mental stress drives vascular inflammation and promotes plaque destabilization in mouse atherosclerosis. *Eur. Heart J.* **42**, 4077–4088 (2021). doi: [10.1093/eurheartj/ehab371](https://doi.org/10.1093/eurheartj/ehab371); pmid: [34279021](https://pubmed.ncbi.nlm.nih.gov/34279021/)
- S. R. Cox *et al.*, Associations between vascular risk factors and brain MRI indices in UK Biobank. *Eur. Heart J.* **40**, 2290–2300 (2019). doi: [10.1093/eurheartj/ezh100](https://doi.org/10.1093/eurheartj/ehz100); pmid: [30854560](https://pubmed.ncbi.nlm.nih.gov/30854560/)
- M. T. Jensen *et al.*, Changes in cardiac morphology and function in individuals with diabetes mellitus: The UK Biobank cardiovascular magnetic resonance substudy. *Circ. Cardiovasc. Imaging* **12**, e009476 (2019). doi: [10.1161/CIRCIMAGING.119.009476](https://doi.org/10.1161/CIRCIMAGING.119.009476); pmid: [31522551](https://pubmed.ncbi.nlm.nih.gov/31522551/)
- S. Subramanipillai *et al.*, Sex- and age-specific associations between cardiometabolic risk and white matter brain age in the UK Biobank cohort. *Hum. Brain Mapp.* **43**, 3759–3774 (2022). doi: [10.1002/hbm.25882](https://doi.org/10.1002/hbm.25882); pmid: [35460147](https://pubmed.ncbi.nlm.nih.gov/35460147/)
- A. G. de Lange *et al.*, Multimodal brain-age prediction and cardiovascular risk: The Whitehall II MRI sub-study. *Neuroimage* **222**, 117292 (2020). doi: [10.1016/j.neuroimage.2020.117292](https://doi.org/10.1016/j.neuroimage.2020.117292); pmid: [32835819](https://pubmed.ncbi.nlm.nih.gov/32835819/)
- M. Babo-Rebelo, C. G. Richter, C. Tallon-Baudry, Neural responses to heartbeats in the default network encode the self in spontaneous thoughts. *J. Neurosci.* **36**, 7829–7840 (2016). doi: [10.1523/JNEUROSCI.0262-16.2016](https://doi.org/10.1523/JNEUROSCI.0262-16.2016); pmid: [27466329](https://pubmed.ncbi.nlm.nih.gov/27466329/)
- S. J. Markovic *et al.*, Investigating the link between later-life brain volume and cardiorespiratory fitness after mild traumatic brain injury exposure. *Gerontology* **69**, 201–211 (2023). doi: [10.1159/000526297](https://doi.org/10.1159/000526297); pmid: [36174542](https://pubmed.ncbi.nlm.nih.gov/36174542/)
- F. Rainaldo *et al.*, Brain-heart interactions reveal consciousness in noncommunicating patients. *Ann. Neurol.* **82**, 578–591 (2017). doi: [10.1002/ana.25045](https://doi.org/10.1002/ana.25045); pmid: [28892566](https://pubmed.ncbi.nlm.nih.gov/28892566/)
- S. E. Petersen *et al.*, UK Biobank's cardiovascular magnetic resonance protocol. *J. Cardiovasc. Magn. Reson.* **18**, 8 (2016). doi: [10.1186/s12968-016-0227-4](https://doi.org/10.1186/s12968-016-0227-4)
- T. J. Littlejohns, C. Sudlow, N. E. Allen, R. Collins, Opportunities for cardiovascular research. *Eur. Heart J.* **40**, 1158–1166 (2019). doi: [10.1093/eurheartj/ehz254](https://doi.org/10.1093/eurheartj/ehz254); pmid: [28531320](https://pubmed.ncbi.nlm.nih.gov/28531320/)
- Z. Raisi-Estabragh, N. C. Harvey, S. Neubauer, S. E. Petersen, Cardiovascular magnetic resonance imaging in the UK Biobank: A major international health research resource. *Eur. Heart J. Cardiovasc. Imaging* **22**, 251–258 (2021). doi: [10.1093/euheartje/jeaa297](https://doi.org/10.1093/euheartje/jeaa297); pmid: [33164079](https://pubmed.ncbi.nlm.nih.gov/33164079/)
- K. L. Miller *et al.*, Multimodal population brain imaging in the UK Biobank prospective epidemiological study. *Nat. Neurosci.* **19**, 1523–1536 (2016). doi: [10.1038/nn.4393](https://doi.org/10.1038/nn.4393); pmid: [27643430](https://pubmed.ncbi.nlm.nih.gov/27643430/)
- M. H. Lee, C. D. Smyser, J. S. Shimony, Resting-state fMRI: A review of methods and clinical applications. *AJR Am. J. Neuroradiol.* **34**, 1866–1872 (2013). doi: [10.3174/ajnr.A3263](https://doi.org/10.3174/ajnr.A3263); pmid: [22936095](https://pubmed.ncbi.nlm.nih.gov/22936095/)
- P. M. Thompson *et al.*, ENIGMA and global neuroscience: A decade of large-scale studies of the brain in health and disease across more than 40 countries. *Transl. Psychiatry* **10**, 100 (2020). doi: [10.1038/s41398-020-0705-1](https://doi.org/10.1038/s41398-020-0705-1); pmid: [32198361](https://pubmed.ncbi.nlm.nih.gov/32198361/)
- G. B. Frisoni, N. C. Fox, C. R. Jack Jr., P. Scheltens, P. M. Thompson, The clinical use of structural MRI in Alzheimer disease. *Nat. Rev. Neurol.* **6**, 67–77 (2010). doi: [10.1038/nrneurop.2009.215](https://doi.org/10.1038/nrneurop.2009.215); pmid: [20313996](https://pubmed.ncbi.nlm.nih.gov/20313996/)
- G. L. Colclough *et al.*, The heritability of multi-modal connectivity in human brain activity. *eLife* **6**, e20178 (2017). doi: [10.7554/eLife.20178](https://doi.org/10.7554/eLife.20178); pmid: [28745584](https://pubmed.ncbi.nlm.nih.gov/28745584/)
- C. A. Busjahn *et al.*, Heritability of left ventricular and papillary muscle heart size: A twin study with cardiac magnetic resonance imaging. *Eur. Heart J.* **30**, 1643–1647 (2009). doi: [10.1093/eurheartj/ehp142](https://doi.org/10.1093/eurheartj/ehp142); pmid: [19406865](https://pubmed.ncbi.nlm.nih.gov/19406865/)
- K.-L. Chien, H.-C. Hsu, T.-C. Su, M.-F. Chen, Y.-T. Lee, Heritability and major gene effects on left ventricular mass in the Chinese population: A family study. *BMC Cardiovasc. Disord.* **6**, 37 (2006). doi: [10.1186/1471-2261-6-37](https://doi.org/10.1186/1471-2261-6-37); pmid: [16945138](https://pubmed.ncbi.nlm.nih.gov/16945138/)
- A. G. Jansen, S. E. Mous, T. White, D. Posthuma, T. J. Polderman, What twin studies tell us about the heritability of brain development, morphology, and function: A review. *Neuropsychol. Rev.* **25**, 27–46 (2015). doi: [10.1007/s11065-015-9278-9](https://doi.org/10.1007/s11065-015-9278-9); pmid: [25672928](https://pubmed.ncbi.nlm.nih.gov/25672928/)
- H. Foo *et al.*, Genetic influence on ageing-related changes in resting-state brain functional networks in healthy adults: A systematic review. *Neurosci. Biobehav. Rev.* **113**, 98–110 (2020). doi: [10.1016/j.neubiorev.2020.03.011](https://doi.org/10.1016/j.neubiorev.2020.03.011); pmid: [32169413](https://pubmed.ncbi.nlm.nih.gov/32169413/)
- N. Aung *et al.*, Genome-wide analysis of left ventricular image-derived phenotypes identifies fourteen loci associated with cardiac morphogenesis and heart failure development. *Circulation* **140**, 1318–1330 (2019). doi: [10.1161/CIRCULATIONAHA.119.041161](https://doi.org/10.1161/CIRCULATIONAHA.119.041161); pmid: [31554410](https://pubmed.ncbi.nlm.nih.gov/31554410/)
- A. Córdoba-Palomera *et al.*, Cardiac imaging of aortic valve area from 34,287 UK Biobank participants reveals novel genetic associations and shared genetic comorbidity with multiple disease phenotypes. *Circ. Genom. Precis. Med.* **13**, e003014 (2020). doi: [10.1161/CIRGEN.120.003014](https://doi.org/10.1161/CIRGEN.120.003014); pmid: [33125279](https://pubmed.ncbi.nlm.nih.gov/33125279/)
- H. V. Meyer *et al.*, Genetic and functional insights into the fractal structure of the heart. *Nature* **584**, 589–594 (2020). doi: [10.1038/s41586-020-2635-8](https://doi.org/10.1038/s41586-020-2635-8); pmid: [32814899](https://pubmed.ncbi.nlm.nih.gov/32814899/)
- J. P. Pirruccello *et al.*, Analysis of cardiac magnetic resonance imaging in 36,000 individuals yields genetic insights into dilated cardiomyopathy. *Nat. Commun.* **11**, 2254 (2020). doi: [10.1038/s41467-020-15823-7](https://doi.org/10.1038/s41467-020-15823-7); pmid: [32382064](https://pubmed.ncbi.nlm.nih.gov/32382064/)
- J. P. Pirruccello *et al.*, Genetic analysis of right heart structure and function in 40,000 people. *Nat. Genet.* **54**, 792–803 (2022). doi: [10.1038/s41588-022-01090-3](https://doi.org/10.1038/s41588-022-01090-3); pmid: [35697867](https://pubmed.ncbi.nlm.nih.gov/35697867/)
- M. Thanaj *et al.*, Genetic and environmental determinants of diastolic heart function. *Nat. Cardiovasc. Res.* **1**, 361–371 (2022). doi: [10.1038/s44161-022-00048-2](https://doi.org/10.1038/s44161-022-00048-2); pmid: [35479509](https://pubmed.ncbi.nlm.nih.gov/35479509/)
- L. T. Elliott *et al.*, Genome-wide association studies of brain imaging phenotypes in UK Biobank. *Nature* **562**, 210–216 (2018). doi: [10.1038/s41586-018-0571-7](https://doi.org/10.1038/s41586-018-0571-7); pmid: [30305740](https://pubmed.ncbi.nlm.nih.gov/30305740/)
- B. Zhao *et al.*, Genome-wide association analysis of 19,629 individuals identifies variants influencing regional brain volumes and refines their genetic co-architecture with cognitive and mental health traits. *Nat. Genet.* **51**, 1637–1644 (2019). doi: [10.1038/s41588-019-0516-6](https://doi.org/10.1038/s41588-019-0516-6); pmid: [31676860](https://pubmed.ncbi.nlm.nih.gov/31676860/)
- S. M. Smith *et al.*, An expanded set of genome-wide association studies of brain imaging phenotypes in UK Biobank. *Nat. Neurosci.* **24**, 737–745 (2021). doi: [10.1038/s41593-021-00826-4](https://doi.org/10.1038/s41593-021-00826-4); pmid: [33875891](https://pubmed.ncbi.nlm.nih.gov/33875891/)
- B. Zhao *et al.*, Common genetic variation influencing human white matter microstructure. *Science* **372**, eabf3736 (2021). doi: [10.1126/science.abf3736](https://doi.org/10.1126/science.abf3736); pmid: [34140357](https://pubmed.ncbi.nlm.nih.gov/34140357/)
- K. L. Grasby *et al.*, The genetic architecture of the human cerebral cortex. *Science* **367**, eaay6690 (2020). doi: [10.1126/science.aaay6690](https://doi.org/10.1126/science.aaay6690); pmid: [32193296](https://pubmed.ncbi.nlm.nih.gov/32193296/)
- B. Zhao *et al.*, Genetic influences on the intrinsic and extrinsic functional organizations of the cerebral cortex. *medRxiv*, 2021.2007.2027.21261187 (2021). doi: [10.1101/2021.07.27.21261187](https://doi.org/10.1101/2021.07.27.21261187)
- E. Hofer *et al.*, Genetic correlations and genome-wide associations of cortical structure in general population samples of 22,824 adults. *Nat. Commun.* **11**, 4796 (2020). doi: [10.1038/s41467-020-18367-y](https://doi.org/10.1038/s41467-020-18367-y); pmid: [32963231](https://pubmed.ncbi.nlm.nih.gov/32963231/)
- C. L. Satizabal *et al.*, Genetic architecture of subcortical brain structures in 38,851 individuals. *Nat. Genet.* **51**, 1624–1636 (2019). doi: [10.1038/s41588-019-0511-y](https://doi.org/10.1038/s41588-019-0511-y); pmid: [31636452](https://pubmed.ncbi.nlm.nih.gov/31636452/)
- B. M. Psaty *et al.*, Cohorts for Heart and Aging Research in Genomic Epidemiology (CHARGE) Consortium: Design of prospective meta-analyses of genome-wide association studies from 5 cohorts. *Circ. Cardiovasc. Genet.* **2**, 73–80 (2009). doi: [10.1161/CIRCGENETICS.108.829747](https://doi.org/10.1161/CIRCGENETICS.108.829747); pmid: [2031568](https://pubmed.ncbi.nlm.nih.gov/2031568)
- L. Mascarell Marićić *et al.*, The IMAGEN study: A decade of imaging genetics in adolescents. *Mol. Psychiatry* **25**, 2648–2671 (2020). doi: [10.1038/s41380-020-0822-5](https://doi.org/10.1038/s41380-020-0822-5); pmid: [32601453](https://pubmed.ncbi.nlm.nih.gov/32601453/)
- T. J. Littlejohns *et al.*, The UK Biobank imaging enhancement of 100,000 participants: Rationale, data collection, management and future directions. *Nat. Commun.* **11**, 2624 (2020). doi: [10.1038/s41467-020-15948-9](https://doi.org/10.1038/s41467-020-15948-9); pmid: [32457287](https://pubmed.ncbi.nlm.nih.gov/32457287/)
- W. Bai *et al.*, A population-based phenotype-wide association study of cardiac and aortic structure and function. *Nat. Med.* **26**, 1654–1662 (2020). doi: [10.1038/s41591-020-1009-y](https://doi.org/10.1038/s41591-020-1009-y); pmid: [32839619](https://pubmed.ncbi.nlm.nih.gov/32839619/)
- W. Bai *et al.*, Automated cardiovascular magnetic resonance image analysis with fully convolutional networks. *J. Cardiovasc. Magn. Reson.* **20**, 65 (2018). doi: [10.1186/s12968-018-0471-x](https://doi.org/10.1186/s12968-018-0471-x); pmid: [30217194](https://pubmed.ncbi.nlm.nih.gov/30217194/)
- W. Bai, H. Suzuki, C. Qin, G. Tarroni, O. Oktay, P. M. Matthews, D. Rueckert, "Recurrent neural networks for aortic image sequence segmentation with sparse annotations," in: A. Frangi, J. Schnabel, C. Davatzikos, C. Alberola-López, G. Fichtinger, Eds. *Medical Image Computing and Computer Assisted Intervention – MICCAI 2018* (Springer, 2018), vol. 11073 of *MICCAI 2018 Lecture Notes in Computer Science*, pp. 586–594.

58. M. D. Cerqueira *et al.*, Standardized myocardial segmentation and nomenclature for tomographic imaging of the heart. A statement for healthcare professionals from the Cardiac Imaging Committee of the Council on Clinical Cardiology of the American Heart Association. *Circulation* **105**, 539–542 (2002). doi: [10.1161/hc0402.102975](https://doi.org/10.1161/hc0402.102975); pmid: [11815441](https://pubmed.ncbi.nlm.nih.gov/11815441/)
59. Supplementary materials are available online.
60. F. Alfaro-Almagro *et al.*, Image processing and Quality Control for the first 10,000 brain imaging datasets from UK Biobank. *Neuroimage* **166**, 400–424 (2018). doi: [10.1016/j.neuroimage.2017.10.034](https://doi.org/10.1016/j.neuroimage.2017.10.034); pmid: [29079522](https://pubmed.ncbi.nlm.nih.gov/29079522/)
61. B. B. Avants *et al.*, A reproducible evaluation of ANTs similarity metric performance in brain image registration. *Neuroimage* **54**, 2033–2044 (2011). doi: [10.1016/j.neuroimage.2010.09.025](https://doi.org/10.1016/j.neuroimage.2010.09.025); pmid: [20851191](https://pubmed.ncbi.nlm.nih.gov/20851191/)
62. S. Mori *et al.*, Stereotaxic white matter atlas based on diffusion tensor imaging in an ICBM template. *Neuroimage* **40**, 570–582 (2008). doi: [10.1016/j.neuroimage.2007.12.035](https://doi.org/10.1016/j.neuroimage.2007.12.035); pmid: [18255316](https://pubmed.ncbi.nlm.nih.gov/18255316/)
63. M. F. Glasser *et al.*, A multi-modal parcellation of human cerebral cortex. *Nature* **536**, 171–178 (2016). doi: [10.1038/nature18933](https://doi.org/10.1038/nature18933); pmid: [27437579](https://pubmed.ncbi.nlm.nih.gov/27437579/)
64. J. L. Ji *et al.*, Mapping the human brain's cortical-subcortical functional network organization. *Neuroimage* **185**, 35–57 (2019). doi: [10.1016/j.neuroimage.2018.10.006](https://doi.org/10.1016/j.neuroimage.2018.10.006); pmid: [30291974](https://pubmed.ncbi.nlm.nih.gov/30291974/)
65. I. J. Bennett, D. J. Madden, C. J. Vaidya, D. V. Howard, J. H. Howard Jr., Age-related differences in multiple measures of white matter integrity: A diffusion tensor imaging study of healthy aging. *Hum. Brain Mapp.* **31**, 378–390 (2010). doi: [10.1002/hbm.20668](https://doi.org/10.1002/hbm.20668)
66. S. M. Smith *et al.*, A positive-negative mode of population covariation links brain connectivity, demographics and behavior. *Nat. Neurosci.* **18**, 1565–1567 (2015). doi: [10.1038/nn.4125](https://doi.org/10.1038/nn.4125); pmid: [26414616](https://pubmed.ncbi.nlm.nih.gov/26414616/)
67. J. Yang, S. H. Lee, M. E. Goddard, P. M. Visscher, GCTA: A tool for genome-wide complex trait analysis. *Am. J. Hum. Genet.* **88**, 76–82 (2011). doi: [10.1016/j.ajhg.2010.11.011](https://doi.org/10.1016/j.ajhg.2010.11.011); pmid: [2167468](https://pubmed.ncbi.nlm.nih.gov/2167468/)
68. B. K. Bulik-Sullivan *et al.*, LD Score regression distinguishes confounding from polygenicity in genome-wide association studies. *Nat. Genet.* **47**, 291–295 (2015). doi: [10.1038/ng.3211](https://doi.org/10.1038/ng.3211); pmid: [25642630](https://pubmed.ncbi.nlm.nih.gov/25642630/)
69. M. Kanai *et al.*, Genetic analysis of quantitative traits in the Japanese population links cell types to complex human diseases. *Nat. Genet.* **50**, 390–400 (2018). doi: [10.1038/s41588-018-0047-6](https://doi.org/10.1038/s41588-018-0047-6); pmid: [29403010](https://pubmed.ncbi.nlm.nih.gov/29403010/)
70. T. S. H. Mak, R. M. Porsch, S. W. Choi, X. Zhou, P. C. Sham, Polygenic scores via penalized regression on summary statistics. *Genet. Epidemiol.* **41**, 469–480 (2017). doi: [10.1002/gepi.22050](https://doi.org/10.1002/gepi.22050); pmid: [28480976](https://pubmed.ncbi.nlm.nih.gov/28480976/)
71. A. Buniello *et al.*, The NHGRI-EBI GWAS Catalog of published genome-wide association studies, targeted arrays and summary statistics 2019. *Nucleic Acids Res.* **47** (D1), D1005–D1012 (2019). doi: [10.1093/nar/gky1120](https://doi.org/10.1093/nar/gky1120); pmid: [30445434](https://pubmed.ncbi.nlm.nih.gov/30445434/)
72. C. Giambartolomei *et al.*, Bayesian test for colocalisation between pairs of genetic association studies using summary statistics. *PLOS Genet.* **10**, e1004383 (2014). doi: [10.1371/journal.pgen.1004383](https://doi.org/10.1371/journal.pgen.1004383); pmid: [24830394](https://pubmed.ncbi.nlm.nih.gov/24830394/)
73. N. K. Kibinge, C. L. Relton, T. R. Gaunt, T. G. Richardson, Characterizing the causal pathway for genetic variants associated with neurological phenotypes using human brain-derived proteome data. *Am. J. Hum. Genet.* **106**, 885–892 (2020). doi: [10.1016/j.ajhg.2020.04.007](https://doi.org/10.1016/j.ajhg.2020.04.007); pmid: [32413284](https://pubmed.ncbi.nlm.nih.gov/32413284/)
74. N. de Klein *et al.*, Brain expression quantitative trait locus and network analyses reveal downstream effects and putative drivers for brain-related diseases. *Nat. Genet.* **55**, 377–388 (2023). doi: [10.1038/s41588-023-01300-6](https://doi.org/10.1038/s41588-023-01300-6); pmid: [36823318](https://pubmed.ncbi.nlm.nih.gov/36823318/)
75. U. Võsa *et al.*, Large-scale cis- and trans-eQTL analyses identify thousands of genetic loci and polygenic scores that regulate blood gene expression. *Nat. Genet.* **53**, 1300–1310 (2021). doi: [10.1038/s41588-021-00913-z](https://doi.org/10.1038/s41588-021-00913-z); pmid: [34475733](https://pubmed.ncbi.nlm.nih.gov/34475733/)
76. C. P. Nelson *et al.*, Association analyses based on false discovery rate implicate new loci for coronary artery disease. *Nat. Genet.* **49**, 1385–1391 (2017). doi: [10.1038/ng.3913](https://doi.org/10.1038/ng.3913); pmid: [28714975](https://pubmed.ncbi.nlm.nih.gov/28714975/)
77. C. Roselli *et al.*, Multi-ethnic genome-wide association study for atrial fibrillation. *Nat. Genet.* **50**, 1225–1233 (2018). doi: [10.1038/s41588-018-0133-9](https://doi.org/10.1038/s41588-018-0133-9); pmid: [29892015](https://pubmed.ncbi.nlm.nih.gov/29892015/)
78. F. Takeuchi *et al.*, Interethnic analyses of blood pressure loci in populations of East Asian and European descent. *Nat. Commun.* **9**, 5052 (2018). doi: [10.1038/s41467-018-07345-0](https://doi.org/10.1038/s41467-018-07345-0); pmid: [30487518](https://pubmed.ncbi.nlm.nih.gov/30487518/)
79. G. T. Jones *et al.*, Meta-analysis of genome-wide association studies for abdominal aortic aneurysm identifies four new disease-specific risk loci. *Circ. Res.* **120**, 341–353 (2017). doi: [10.1161/CIRCRESAHA.116.308765](https://doi.org/10.1161/CIRCRESAHA.116.308765); pmid: [27899403](https://pubmed.ncbi.nlm.nih.gov/27899403/)
80. C. Dina *et al.*, Genetic association analyses highlight biological pathways underlying mitral valve prolapse. *Nat. Genet.* **47**, 1206–1211 (2015). doi: [10.1038/ng.3383](https://doi.org/10.1038/ng.3383); pmid: [26301497](https://pubmed.ncbi.nlm.nih.gov/26301497/)
81. E. Villard *et al.*, A genome-wide association study identifies two loci associated with heart failure due to dilated cardiomyopathy. *Eur. Heart J.* **32**, 1065–1076 (2011). doi: [10.1093/eurheartj/ehr105](https://doi.org/10.1093/eurheartj/ehr105); pmid: [21459883](https://pubmed.ncbi.nlm.nih.gov/21459883/)
82. R. Malik *et al.*, Multiancestry genome-wide association study of 520,000 subjects identifies 32 loci associated with stroke and stroke subtypes. *Nat. Genet.* **50**, 524–537 (2018). doi: [10.1038/s41588-018-0058-3](https://doi.org/10.1038/s41588-018-0058-3); pmid: [29531354](https://pubmed.ncbi.nlm.nih.gov/29531354/)
83. T. Foroud *et al.*, Genome-wide association study of intracranial aneurysm identifies a new association on chromosome 7. *Stroke* **45**, 3194–3199 (2014). doi: [10.1161/STROKEAHA.114.006096](https://doi.org/10.1161/STROKEAHA.114.006096); pmid: [25256182](https://pubmed.ncbi.nlm.nih.gov/25256182/)
84. L. Duan *et al.*, Novel susceptibility loci for moyamoya disease revealed by a genome-wide association study. *Stroke* **49**, 11–18 (2018). doi: [10.1161/STROKEAHA.117.017430](https://doi.org/10.1161/STROKEAHA.117.017430); pmid: [2973593](https://pubmed.ncbi.nlm.nih.gov/2973593/)
85. M. A. Tischfield *et al.*, Cerebral vein malformations result from loss of Twist1 expression and BMP signaling from skull progenitor cells and dura. *Dev. Cell* **42**, 445–461.e5 (2017). doi: [10.1016/j.devcel.2017.07.027](https://doi.org/10.1016/j.devcel.2017.07.027); pmid: [28844842](https://pubmed.ncbi.nlm.nih.gov/28844842/)
86. Y. D'Souza, A. Elharram, R. Soon-Shiong, R. D. Andrew, B. M. Bennett, Characterization of Aldh2 (-/-) mice as an age-related model of cognitive impairment and Alzheimer's disease. *Mol. Brain* **8**, 27 (2015). doi: [10.1186/s13041-015-0117-y](https://doi.org/10.1186/s13041-015-0117-y); pmid: [25910195](https://pubmed.ncbi.nlm.nih.gov/25910195/)
87. J. Simón-Sánchez *et al.*, Genome-wide association study reveals genetic risk underlying Parkinson's disease. *Nat. Genet.* **41**, 1308–1312 (2009). doi: [10.1038/ng.487](https://doi.org/10.1038/ng.487); pmid: [19195575](https://pubmed.ncbi.nlm.nih.gov/19195575/)
88. M. I. Kamboh *et al.*, Genome-wide association study of Alzheimer's disease. *Transl. Psychiatry* **2**, e117 (2012). doi: [10.1038/tp.2012.45](https://doi.org/10.1038/tp.2012.45); pmid: [22832961](https://pubmed.ncbi.nlm.nih.gov/22832961/)
89. P. T. Nelson *et al.*, ABCG9 gene polymorphism is associated with hippocampal sclerosis of aging pathology. *Acta Neuropathol.* **127**, 825–843 (2014). doi: [10.1007/s00401-014-1282-2](https://doi.org/10.1007/s00401-014-1282-2); pmid: [24770881](https://pubmed.ncbi.nlm.nih.gov/24770881/)
90. A. F. Pardiñas *et al.*, Common schizophrenia alleles are enriched in mutation-intolerant genes and in regions under strong background selection. *Nat. Genet.* **50**, 381–389 (2018). doi: [10.1038/s41588-018-0059-2](https://doi.org/10.1038/s41588-018-0059-2); pmid: [29483656](https://pubmed.ncbi.nlm.nih.gov/29483656/)
91. L. Hou *et al.*, Genome-wide association study of 40,000 individuals identifies two novel loci associated with bipolar disorder. *Hum. Mol. Genet.* **25**, 3383–3394 (2016). doi: [10.1093/hmg/ddw181](https://doi.org/10.1093/hmg/ddw181); pmid: [27329760](https://pubmed.ncbi.nlm.nih.gov/27329760/)
92. T. D. Wade *et al.*, Genetic variants associated with disordered eating. *Int. J. Eat. Disord.* **46**, 594–608 (2013). doi: [10.1002/eat.22133](https://doi.org/10.1002/eat.22133); pmid: [23568457](https://pubmed.ncbi.nlm.nih.gov/23568457/)
93. Z. Raisi-Estabragh *et al.*, Associations of cognitive performance with cardiovascular magnetic resonance phenotypes in the UK Biobank. *Eur. Heart J. Cardiovasc. Imaging* **23**, 663–672 (2022). doi: [10.1093/eihci/jeab075](https://doi.org/10.1093/eihci/jeab075); pmid: [33987659](https://pubmed.ncbi.nlm.nih.gov/33987659/)
94. R. F. Gottesman *et al.*, Associations between midlife vascular risk factors and 25-year incident dementia in the Atherosclerosis Risk in Communities (ARIC) cohort. *JAMA Neurol.* **74**, 1246–1254 (2017). doi: [10.1001/jamaneurol.2017.1658](https://doi.org/10.1001/jamaneurol.2017.1658); pmid: [28783817](https://pubmed.ncbi.nlm.nih.gov/28783817/)
95. V. Vaccarino *et al.*, Brain-heart connections in stress and cardiovascular disease: Implications for the cardiac patient. *Atherosclerosis* **328**, 74–82 (2021). doi: [10.1016/j.atherosclerosis.2021.05.020](https://doi.org/10.1016/j.atherosclerosis.2021.05.020); pmid: [34102426](https://pubmed.ncbi.nlm.nih.gov/34102426/)
96. J. C. Barrett *et al.*, Genome-wide association study and meta-analysis find that over 40 loci affect risk of type 1 diabetes. *Nat. Genet.* **41**, 703–707 (2009). doi: [10.1038/ng.381](https://doi.org/10.1038/ng.381); pmid: [19430480](https://pubmed.ncbi.nlm.nih.gov/19430480/)
97. D. L. Cousminer *et al.*, First genome-wide association study of latent autoimmune diabetes in adults reveals novel insights linking immune and metabolic diabetes. *Diabetes Care* **41**, 2396–2403 (2018). doi: [10.2337/dc18-1032](https://doi.org/10.2337/dc18-1032); pmid: [30254083](https://pubmed.ncbi.nlm.nih.gov/30254083/)
98. A. Mahajan *et al.*, Multi-ancestry genetic study of type 2 diabetes highlights the power of diverse populations for discovery and translation. *Nat. Genet.* **54**, 560–572 (2022). doi: [10.1038/s41588-022-01058-3](https://doi.org/10.1038/s41588-022-01058-3); pmid: [35551307](https://pubmed.ncbi.nlm.nih.gov/35551307/)
99. F. Demenais *et al.*, Multiancestry association study identifies new asthma risk loci that colocalize with immune-cell enhancer marks. *Nat. Genet.* **50**, 42–53 (2018). doi: [10.1038/s41588-017-0014-7](https://doi.org/10.1038/s41588-017-0014-7); pmid: [29273806](https://pubmed.ncbi.nlm.nih.gov/29273806/)
100. I. Noth *et al.*, Genetic variants associated with idiopathic pulmonary fibrosis susceptibility and mortality: A genome-wide association study. *Lancet Respir. Med.* **1**, 309–317 (2013). doi: [10.1016/S2213-2600\(13\)70045-6](https://doi.org/10.1016/S2213-2600(13)70045-6); pmid: [24429156](https://pubmed.ncbi.nlm.nih.gov/24429156/)
101. T. E. Fingerlin *et al.*, Genome-wide association study identifies multiple susceptibility loci for pulmonary fibrosis. *Nat. Genet.* **45**, 613–620 (2013). doi: [10.1038/ng.2609](https://doi.org/10.1038/ng.2609); pmid: [23583980](https://pubmed.ncbi.nlm.nih.gov/23583980/)
102. B. Bulik-Sullivan *et al.*, An atlas of genetic correlations across human diseases and traits. *Nat. Genet.* **47**, 1236–1241 (2015). doi: [10.1038/ng.3406](https://doi.org/10.1038/ng.3406); pmid: [26414676](https://pubmed.ncbi.nlm.nih.gov/26414676/)
103. S. Burgess, F. Dudbridge, S. G. Thompson, Combining information on multiple instrumental variables in Mendelian randomization: Comparison of allele score and summarized data methods. *Stat. Med.* **35**, 1880–1906 (2016). doi: [10.1002/sim.6835](https://doi.org/10.1002/sim.6835); pmid: [26661904](https://pubmed.ncbi.nlm.nih.gov/26661904/)
104. M. I. Kurki *et al.*, FinnGen provides genetic insights from a well-phenotyped isolated population. *Nature* **613**, 508–518 (2023). doi: [10.1038/s41586-022-0547-8](https://doi.org/10.1038/s41586-022-0547-8); pmid: [36653562](https://pubmed.ncbi.nlm.nih.gov/36653562/)
105. P. F. Sullivan *et al.*, Psychiatric genomics: An update and an agenda. *Am. J. Psychiatry* **175**, 15–27 (2018). doi: [10.1176/appi.ajph.2017.17030283](https://doi.org/10.1176/appi.ajph.2017.17030283); pmid: [28964422](https://pubmed.ncbi.nlm.nih.gov/28964422/)
106. Cross-Disease Group of the Psychiatric Genomics Consortium, Identification of risk loci with shared effects on five major psychiatric disorders: A genome-wide analysis. *Lancet* **381**, 1371–1379 (2013). doi: [10.1016/S0140-6736\(12\)62129-1](https://doi.org/10.1016/S0140-6736(12)62129-1); pmid: [23453885](https://pubmed.ncbi.nlm.nih.gov/23453885/)
107. A. K. Dhar, D. A. Barton, Depression and the link with cardiovascular disease. *Front. Psychiatry* **7**, 33 (2016). doi: [10.3389/fpsyti.2016.00033](https://doi.org/10.3389/fpsyti.2016.00033); pmid: [27047396](https://pubmed.ncbi.nlm.nih.gov/27047396/)
108. H. L. Hu *et al.*, Association between depression and clinical outcomes in patients with hypertrophic cardiomyopathy. *J. Am. Heart Assoc.* **10**, e019071 (2021). doi: [10.1161/JAHA.120.019071](https://doi.org/10.1161/JAHA.120.019071); pmid: [33834850](https://pubmed.ncbi.nlm.nih.gov/33834850/)
109. J. F. Morgan, A. C. O'Donoghue, W. J. McKenna, M. M. Schmidt, Psychiatric disorders in hypertrophic cardiomyopathy. *Gen. Hosp. Psychiatry* **30**, 49–54 (2008). doi: [10.1016/j.genhosppsych.2007.09.005](https://doi.org/10.1016/j.genhosppsych.2007.09.005); pmid: [18164940](https://pubmed.ncbi.nlm.nih.gov/18164940/)
110. C. Cuspidi, M. Tadic, Obstructive sleep apnea and left ventricular strain: Useful tool or fancy gadget? *J. Clin. Hypertens. (Greenwich)* **22**, 120–122 (2020). doi: [10.1111/jch.13787](https://doi.org/10.1111/jch.13787); pmid: [31891443](https://pubmed.ncbi.nlm.nih.gov/31891443/)
111. C. A. de Leeuw, J. M. Mooij, T. Heskes, D. Posthuma, MAGMA: Generalized gene-set analysis of GWAS data. *PLOS Comput. Biol.* **11**, e1004219 (2015). doi: [10.1371/journal.pcbi.1004219](https://doi.org/10.1371/journal.pcbi.1004219); pmid: [25885710](https://pubmed.ncbi.nlm.nih.gov/25885710/)
112. K. Watanabe, E. Taskesen, A. van Bochoven, D. Posthuma, Functional mapping and annotation of genetic associations with FUMA. *Nat. Commun.* **8**, 1826 (2017). doi: [10.1038/s41467-017-01261-5](https://doi.org/10.1038/s41467-017-01261-5); pmid: [29184056](https://pubmed.ncbi.nlm.nih.gov/29184056/)
113. M. Lek *et al.*, Analysis of protein-coding genetic variation in 60,706 humans. *Nature* **536**, 285–291 (2016). doi: [10.1038/nature19057](https://doi.org/10.1038/nature19057); pmid: [27535533](https://pubmed.ncbi.nlm.nih.gov/27535533/)
114. H. K. Finucane *et al.*, Partitioning heritability by functional annotation using genome-wide association summary statistics. *Nat. Genet.* **47**, 1228–1235 (2015). doi: [10.1038/ng.3404](https://doi.org/10.1038/ng.3404); pmid: [26414678](https://pubmed.ncbi.nlm.nih.gov/26414678/)
115. A. Kundaje *et al.*, Integrative analysis of 111 reference human epigenomes. *Nature* **518**, 317–330 (2015). doi: [10.1038/nature14248](https://doi.org/10.1038/nature14248); pmid: [25693563](https://pubmed.ncbi.nlm.nih.gov/25693563/)
116. Q. Wang *et al.*, A Bayesian framework that integrates multi-omics data and gene networks predicts risk genes from schizophrenia GWAS data. *Nat. Neurosci.* **22**, 691–699 (2019). doi: [10.1038/s41593-019-0382-7](https://doi.org/10.1038/s41593-019-0382-7); pmid: [30988527](https://pubmed.ncbi.nlm.nih.gov/30988527/)
117. X.-J. Luo, B. Liu, Q.-L. Ma, J. Peng, Mitochondrial aldehyde dehydrogenase, a potential drug target for protection of heart and brain from ischemia/reperfusion injury. *Curr. Drug Targets* **15**, 948–955 (2014). doi: [10.2174/13894501566614082814201](https://doi.org/10.2174/13894501566614082814201); pmid: [25163552](https://pubmed.ncbi.nlm.nih.gov/25163552/)
118. J. Pang, J. Wang, Y. Zhang, F. Xu, Y. Chen, Targeting acetaldehyde dehydrogenase 2 (ALDH2) in heart failure: Recent insights and perspectives. *Biochim. Biophys. Acta Mol. Basis Dis.* **1863**, 1933–1941 (2017). doi: [10.1016/j.bbapap.2016.10.004](https://doi.org/10.1016/j.bbapap.2016.10.004); pmid: [27742538](https://pubmed.ncbi.nlm.nih.gov/27742538/)
119. C.-H. Chen, J. C. B. Ferreira, E. R. Gross, D. Mochly-Rosen, Targeting aldehyde dehydrogenase 2: New therapeutic opportunities. *Physiol. Rev.* **94**, 1–34 (2014). doi: [10.1152/physrev.00017.2013](https://doi.org/10.1152/physrev.00017.2013); pmid: [24382882](https://pubmed.ncbi.nlm.nih.gov/24382882/)

120. E. C. Ballinger, M. Ananth, D. A. Talmage, L. W. Role, Basal forebrain cholinergic circuits and signaling in cognition and cognitive decline. *Neuron* **91**, 1199–1218 (2016). doi: [10.1016/j.neuron.2016.09.006](https://doi.org/10.1016/j.neuron.2016.09.006); pmid: [27657448](https://pubmed.ncbi.nlm.nih.gov/27657448/)
121. C. Geula *et al.*, Basal forebrain cholinergic system in the dementias: Vulnerability, resilience, and resistance. *J. Neurochem.* **158**, 1394–1411 (2021). doi: [10.1111/jnc.15471](https://doi.org/10.1111/jnc.15471); pmid: [34272732](https://pubmed.ncbi.nlm.nih.gov/34272732/)
122. Y. Iturria-Medina, R. C. Sotero, P. J. Toussaint, J. M. Mateos-Pérez, A. C. Evans, Alzheimer's Disease Neuroimaging Initiative, Early role of vascular dysregulation on late-onset Alzheimer's disease based on multifactorial data-driven analysis. *Nat. Commun.* **7**, 11934 (2016). doi: [10.1038/ncomms11934](https://doi.org/10.1038/ncomms11934); pmid: [27327500](https://pubmed.ncbi.nlm.nih.gov/27327500/)
123. T. W. Schmitz, R. Nathan Spreng, Alzheimer's Disease Neuroimaging Initiative, Basal forebrain degeneration precedes and predicts the cortical spread of Alzheimer's pathology. *Nat. Commun.* **7**, 13249 (2016). doi: [10.1038/ncomms13249](https://doi.org/10.1038/ncomms13249); pmid: [27811848](https://pubmed.ncbi.nlm.nih.gov/27811848/)
124. J. C. Huffman, T. A. Stern, Neuropsychiatric consequences of cardiovascular medications. *Dialogues Clin. Neurosci.* **9**, 29–45 (2007). doi: [10.31887/DCNS.2007.9.1/jchuffman](https://doi.org/10.31887/DCNS.2007.9.1/jchuffman); pmid: [17506224](https://pubmed.ncbi.nlm.nih.gov/17506224/)
125. M. Stuhec, J. Keuschler, J. Serra-Mestres, M. Isetta, Effects of different antihypertensive medication groups on cognitive function in older patients: A systematic review. *Eur. Psychiatry* **46**, 1–15 (2017). doi: [10.1016/j.eurpsy.2017.07.015](https://doi.org/10.1016/j.eurpsy.2017.07.015); pmid: [28992530](https://pubmed.ncbi.nlm.nih.gov/28992530/)
126. Y.-N. Ou *et al.*, Blood pressure and risks of cognitive impairment and dementia: A systematic review and meta-analysis of 209 prospective studies. *Hypertension* **76**, 217–225 (2020). doi: [10.1161/HYPERTENSIONAHA.120.14993](https://doi.org/10.1161/HYPERTENSIONAHA.120.14993); pmid: [32450739](https://pubmed.ncbi.nlm.nih.gov/32450739/)
127. L. Colbourne, P. J. Harrison, Brain-penetrant calcium channel blockers are associated with a reduced incidence of neuropsychiatric disorders. *Mol. Psychiatry* **27**, 3904–3912 (2022). doi: [10.1038/s41380-022-01615-6](https://doi.org/10.1038/s41380-022-01615-6); pmid: [35618884](https://pubmed.ncbi.nlm.nih.gov/35618884/)
128. G. de Simone, M. Galderisi, Allometric normalization of cardiac measures: Producing better, but imperfect, accuracy. *J. Am. Soc. Echocardiogr.* **27**, 1275–1278 (2014). doi: [10.1016/j.echo.2014.10.006](https://doi.org/10.1016/j.echo.2014.10.006); pmid: [25479898](https://pubmed.ncbi.nlm.nih.gov/25479898/)
129. A. L. Alexander, J. E. Lee, M. Lazar, A. S. Field, Diffusion tensor imaging of the brain. *Neurotherapeutics* **4**, 316–329 (2007). doi: [10.1016/j.nurt.2007.05.011](https://doi.org/10.1016/j.nurt.2007.05.011); pmid: [17599699](https://pubmed.ncbi.nlm.nih.gov/17599699/)
130. L. K. Ferreira, G. F. Busatto, Resting-state functional connectivity in normal brain aging. *Neurosci. Biobehav. Rev.* **37**, 384–400 (2013). doi: [10.1016/j.neubiorev.2013.01.017](https://doi.org/10.1016/j.neubiorev.2013.01.017); pmid: [23333262](https://pubmed.ncbi.nlm.nih.gov/23333262/)
131. A. Fry *et al.*, Comparison of sociodemographic and health-related characteristics of UK Biobank participants with those of the general population. *Am. J. Epidemiol.* **186**, 1026–1034 (2017). doi: [10.1093/aje/kwx246](https://doi.org/10.1093/aje/kwx246); pmid: [28641372](https://pubmed.ncbi.nlm.nih.gov/28641372/)
132. A. R. Laird, Large, open datasets for human connectomics research: Considerations for reproducible and responsible data use. *Neuroimage* **244**, 118579 (2021). doi: [10.1016/j.neuroimage.2021.118579](https://doi.org/10.1016/j.neuroimage.2021.118579); pmid: [34536537](https://pubmed.ncbi.nlm.nih.gov/34536537/)
133. C. McCracken *et al.*, Multorgan imaging demonstrates the heart-brain-liver axis in UK Biobank participants. *Nat. Commun.* **13**, 7839 (2022). doi: [10.1038/s41467-022-35321-2](https://doi.org/10.1038/s41467-022-35321-2); pmid: [36543768](https://pubmed.ncbi.nlm.nih.gov/36543768/)
134. M. Carabotti, A. Scirocco, M. A. Maselli, C. Severi, The gut-brain axis: Interactions between enteric microbiota, central and enteric nervous systems. *Ann. Gastroenterol.* **28**, 203–209 (2015). pmid: [25830558](https://pubmed.ncbi.nlm.nih.gov/25830558/)
135. B. Barberio, M. Zamani, C. J. Black, E. V. Savarino, A. C. Ford, Prevalence of symptoms of anxiety and depression in patients with inflammatory bowel disease: A systematic review and meta-analysis. *Lancet Gastroenterol. Hepatol.* **6**, 359–370 (2021). doi: [10.1016/S2468-1253\(21\)00014-5](https://doi.org/10.1016/S2468-1253(21)00014-5); pmid: [33721557](https://pubmed.ncbi.nlm.nih.gov/33721557/)
136. L. Jiang *et al.*, A resource-efficient tool for mixed model association analysis of large-scale data. *Nat. Genet.* **51**, 1749–1755 (2019). doi: [10.1038/s41588-019-0530-8](https://doi.org/10.1038/s41588-019-0530-8); pmid: [31768069](https://pubmed.ncbi.nlm.nih.gov/31768069/)
137. Analysis code for: B. Zhao *et al.*, Heart-brain connections: phenotypic and genetic insights from magnetic resonance images. Zenodo (2023); <https://zenodo.org/record/7799207>.
138. GWAS summary statistics for: B. Zhao *et al.*, Heart-brain connections: phenotypic and genetic insights from magnetic resonance images. Zenodo (2023); <https://zenodo.org/record/7239166>.

#### ACKNOWLEDGMENTS

We thank the individuals represented in the UKB for their participation and the research teams for their work in collecting, processing, and disseminating these datasets for analysis; the research computing groups at the University of North Carolina at Chapel Hill, Purdue University, and the Wharton School of the University of Pennsylvania for providing computational resources and support that have contributed to these research results; and all of the authors and databases that made GWAS and eQTL summary-level data publicly available. **Funding:** This research was partially supported by National Institutes of Health (grant

MH086633 to H.Z., grant MH116527 to T.F.L., and grant R56 AG079291 to Y.L.; startup funding from Purdue University Department of Statistics (B.Z.); and the UNC Intellectual and Developmental Disabilities Research Center (Eunice Kennedy Shriver National Institute of Child Health and Human Development grant P50 HD103573 to Y.L.). This research was conducted using the UKB resource (application no. 22783), which is subject to a data transfer agreement. **Author contributions:** B.Z. designed the study. B.Z., T.F.L., Z.F., Y.Y., J.S., X.Y., X.W., T.Y.L., J.T., D.X., Z.W., and B.L. analyzed the data. T.F.L., Y.Y., J.T., X.W., D.X., T.Y.L., J.C., Y.S., C.T., and Z.Z. processed heart imaging data and undertook quantity controls. H.Z., J.L.S., and Y.L. provided feedback on the study design and results interpretation. B.Z. wrote the manuscript with contributions from J.S. and X.Y. and feedback from all authors. **Competing interests:** Chalmer Tomlinson is currently an employee at Janssen R&D of Johnson & Johnson, Raritan, NJ, USA. The remaining authors declare that no competing interests. **Data and materials availability:** We made use of publicly available software and tools. Our analysis code is freely available at Zenodo ([137](https://doi.org/10.5281/zenodo.5400000)). The code for heart image analysis can be found at [https://github.com/bawenjia/ukbb\\_cardiac](https://github.com/bawenjia/ukbb_cardiac). The code for CCA can be found at <https://www.fmrib.ox.ac.uk/datasets/HCP-CCA/>. Our GWAS summary statistics of 82 CMR traits have been shared on Zenodo ([138](https://doi.org/10.5281/zenodo.5400000)) and at Heart-KP (<http://heartkp.org/>). The GWAS summary statistics of brain MRI traits can be freely downloaded at BIG-KP <https://bigkp.org/>. The individual-level UKB data used in this study can be obtained from <https://www.ukbiobank.ac.uk/>. **License information:** Copyright © 2023 the authors, some rights reserved; exclusive licensee American Association for the Advancement of Science. No claim to original US government works. <https://www.science.org/about/science-licenses-journal-article-reuse>

#### SUPPLEMENTARY MATERIALS

[science.org/doi/10.1126/science.abn6598](https://science.org/doi/10.1126/science.abn6598)

Materials and Methods

Supplementary Text

Figs. S1 to S117

Tables S1 to S20

References ([139–156](https://doi.org/10.1126/science.abn6598))

MDAR Reproducibility Checklist

[View/request a protocol for this paper from Bio-protocol.](https://science.org/about/science-licenses-journal-article-reuse)

Submitted 10 December 2021; resubmitted 17 November 2022

Accepted 11 April 2023

10.1126/science.abn6598